New Results on Selection Diversity Over Fading Channels

By

Qiang Zhao

Thesis submitted to the faculty of

Virginia Polytechnic Institute and State University

in partial fulfillment of the requirements for the degree of

Master of Science

In

Electrical Engineering

Dr. Annamalai Annamalai, Chair

Dr. Jeffrey H. Reed

Dr. William H. Tranter

December 27, 2002

Blacksburg, Virginia

Keywords: low-complexity receiver design, diversity reception, multipath fading

New Results on Selection Diversity Over Fading Channels

Qiang Zhao

(Abstract)

This thesis develops a mathematical framework for analyzing the average bit error rate performance of five different selection diversity combining schemes over slow, frequency non-selective Rayleigh, Nakagami-*m* and Ricean fading channels. Aside from the classical selection diversity, generalized selection combining and the "maximum output" selection methods, two new selection rules based on choosing the branch providing the largest magnitude of log-likelihood ratio for binary phase shift keying signals (with and without phase compensation in the selection process) are also investigated. The proposed analytical framework is sufficiently general to study the effects of dissimilar fading parameter and unequal mean received signal strengths across the independent diversity paths. The effect of branch correlation on the performance of a dual-diversity system is also studied. The accuracies of our analytical expressions have been validated by extensive Monte-Carlo simulation runs. The proposed selection schemes based on the log-likelihood ratio are attractive in the design of low-complexity rake receivers for wideband CDMA and ultra wideband communication systems.

ACKNOWLEDGEMENTS

First of all, I would like to thank my thesis advisor, Dr. A. Annamalai, for his invaluable support and guidance during the course of this research. I am grateful to Dr. William H. Tranter and Dr. Jeffrey H. Reed for agreeing to be on my thesis committee and reviewing my research work.

I would also like to thank the students and staff of Mobile and Portable Radio Research Group (MPRG) who assisted me through my thesis. Special thank goes to Gautam for his helpful suggestions on my work.

Finally, I would like to thank my wife, Jihong, my parents, Chongxi and Ruoxia, for their love and continuous support during my academic studies.

CONTENTS

LIST OF FIGURES

Chapter 1

INTRODUCTION

Many of the current and emerging wireless communication systems make use of diversity in their design: a classic and well-known concept that has been used for the past half century to combat the detrimental effects of multipath fading. Indeed, diversity techniques at the receiver, in which two or more copies of the same information-bearing signal are combined skillfully to increase the overall signal-to-noise ratio (SNR), still offer one of the greatest potential for radio link performance improvement to many of the current and future wireless technologies. For example, to meet stringent requirements for quality service requirements and spectrally efficient multilevel constellations, antenna (space) diversity is needed to offset penalty on the SNR due to fading and denser signal constellation. In addition, one of the most promising features of wideband code division multiple access (CDMA) systems is their ability to resolve additional multipaths (compared to "narrowband" CDMA systems), resulting in an increased multipath diversity which can be exploited by rake reception. There are several ways in which we can provide the receiver with an L-order diversity (i.e., fading replicas of the same information-bearing signal).

- Space diversity

Space diversity consists of receiving the transmitted signal through L separate antennas, whose spacing is wide enough with respect to the carrier wavelength so as to obtain sufficient decorrelation. This technique can be easily implemented at the base stations, and does not require extra radio spectrum occupancy.

- Frequency diversity

This form of diversity is obtained by sending the same signal over different frequency carriers, whose separation should be larger than the coherence bandwidth of the channel. Clearly, frequency diversity is not a bandwidth efficient solution.

- Time diversity

If the same information bearing signals are transmitted in different time slots separated by an interval longer than the coherence time of the channel, time diversity can be obtained.

1.1 Overview of Diversity Combining Techniques

As mentioned above, diversity has long been recognized as a powerful communication receiver technique for mitigating the detrimental effects of channel fading and co-channel interference. The underlying premise is that if several uncorrelated replicas of a signal are received over multiple diversity paths with comparable signal strengths, then it is improbable that these signals will experience simultaneous deep fades. Diversity methods can be employed either at the base station (macroscopic diversity) or at the mobile station (microscopic diversity), although the antenna separation required differs for each case. In practice, microscopic diversity reception techniques are employed to combat the fast fading variations in the received signal strength caused by fast fading, whereas macroscopic diversity is used to mitigate the slower fading variations caused by shadowing. A thorough treatment of the diversity schemes and the signal combining techniques may be found in [1]-[3].

Diversity schemes can be classified according to the type of combining employed at the receiver, namely, maximal-ratio combining (MRC), equal gain combining (EGC), selection diversity combining (SDC) and generalized selection combining (GSC). In MRC, the voltage signals from each of the L diversity branch are co-phased to provide coherent voltage addition and are individually weighted to provide SNR of the combiner, MRC is known to be optimum in the sense that it yields the best statistical reduction of fading in any linear diversity combiner. A number or researchers have analyzed the performance of MRC systems over Nakagami-*m* fading channels [4]-[6].

In an EGC combiner, the outputs of different diversity branches are first co-phased and weighted equally before being summed to give the resultant output [7]-[9]. EGC combiner does not require the estimation of the channel gains, and hence it results in reduced receiver complexity relative to the MRC scheme. However, the performance of EGC is inferior to that of MRC since the branch weights are all set to unity.

SDC scheme, which selects the branch that provides the highest instantaneous SNR[10]-[11], is the simplest and perhaps the most frequently used form of diversity combining. However, this is achieved at the expense of receiver performance (i.e., SDC is inferior to the MRC and EGC schemes).

The complexity of MRC and EGC receivers depends on the number of diversity paths available, which can be quite high, especially for multipath diversity of wideband CDMA and ultra wideband (UWB) signals. In addition, MRC is sensitive to channel estimation errors, and these errors tend to be more important when the SNR is low. On the other hand, SDC scheme uses only one path out of the L available multipaths. Consequently, it does not fully exploit the amount of diversity offered by the channel. Recently, a wave of papers have been published to bridge the gap between these two extremes (MRC/EGC and SDC) by proposing GSC scheme[12]-[15]. The GSC receiver (hereafter, referred to as α -GSC) adaptively combines a subset of N strongest multipaths (highest SNR) among the L available paths.

The traditional selection diversity combining (hereafter, referred to as α -SDC) measures the signal-to-noise ratio at each path and chooses the path with the highest SNR for data recovery. However, in practice, the measurements of SNR may not be trivial, especially for high data rate transmissions. To be most effective, the system should be able to make its selection in a period of time equal to or less than the interval of the shortest signal that will be transmitted. Consequently, the branch with the largest amplitude of the received composite signal (i.e., matched filter output) is chosen. This is the main motivation behind the development of "maximum-output" SDC scheme [16]-18] (hereafter, referred to as r-SDC).

1.2 Motivation for Research

In [16], Chyi et al. investigated the performance of two receiver structures for non-coherent M-ary orthogonal frequency shift keying (FSK) over slow frequency non-selective Rayleigh fading channels. They have shown that α-SDC has inferior performance compared to that of r-SDC. The analysis was extended in [17] by considering four receiver structures for non-coherent binary orthogonal FSK and two receiver structures for differential binary phase shift keying (BPSK), also in a Rayleigh fading environment. Furthermore, an explanation for the rather interesting observation cited in [16] was furnished, with the reason being that α-SDC does not take into account of the stochastic nature of the noise. Ref. [18] validates the observations cited in [16]-[17], but for the coherent BPSK case and in Nakagami-m channels. Moreover, [18] points out that r-SDC exhibits comparable performance with that of the optimal linear MRC in good channel conditions (less severe than Rayleigh fading) and small diversity orders. Nevertheless, we should keep in mind that these conclusions were drawn based on the assumption that all the statistically independent diversity paths have identical fading statistics (i.e., equal mean received signal strengths and identical fading severity index).

Recently Kim et al. [19] proposed a new selection diversity rule (hereafter, referred to as αr-SDC) for BPSK that selects the diversity path providing the largest magnitude of log-likelihood ratio (LLR) in a Rayleigh fading environment with independent and identically distributed (i.i.d) diversity paths. It is shown that the LLR for BPSK signals in fading channels is proportional to the product of the fading amplitude and the magnitude of the matched filter output. This selection rule is optimum in the sense that it minimizes the average bit error rate (ABER) among all SDC schemes. Ref. [19] also investigates the performance of a suboptimal SDC scheme which does not require phase compensation in the selection process (hereafter, referred to as αw-SDC) via simulation.

The αr-SDC and αw-SDC schemes find their potential application in the design of low-complexity receiver structures for wideband cellular CDMA and UWB communication systems. For instance, the pulse width is extremely short (usually in the order of picoseconds) for ultra wideband signals, this yields a large number of resolvable multipaths at the rake receiver input. To exploit the benefit of diversity as well as capture significant amount of energy available in the multipaths, one need to design a rake receiver with a large number of taps (rake fingers), resulting in increased complexity. Both αr-SDC and αw-SDC facilitate the design of low-complexity receiver structures, while ensuring graceful degradation of ABER performance with fewer rake fingers.

1.3 Contribution of Thesis

In this thesis, we extend the analysis presented in [19] in several fronts: First, we move away from the restriction of independent and identically distributed (i.i.d) fading statistics and study the effectiveness of αr-SDC and αw-SDC selection rules in a more realistic (practical) operating environments. Due to the random nature of the propagation channel, it is more realistic to assume that the mean received signal strengths and/or the fading severity index may be different for the different diversity paths. This may well be the case in an actual mobile link, since the radio waves take different propagation paths and may undergo different amount of fading before arriving at the receiver. Specifically, we derive analytical expressions for evaluating the αr-SDC performance over Rayleigh, Nakagami-*m* and Ricean fading channels with independent but non-identically distributed (i.n.d) diversity paths. Secondly, we study the effect of branch correlations on the performance of αr-SDC, αw-SDC and *r*-SDC receiver structures. In addition to the αr-SDC and αw-SDC selection methods, performances of MRC, α-SDC, *r*-SDC, and α-GSC are also evaluated for comparison. Finally, the performances of αr-SDC and αw-SDC are evaluated in the context of Vehicular A UMTS WCDMA channel model, and compared against that of currently implemented α-GSC receiver structure.

1.4 Outline of Thesis

The remainder of this thesis is organized as follows: A brief description of the system model is provided in Chapter 2. Chapter 3 details the average bit error rate analysis for αr-SDC, α-SDC, *r*-SDC and α-GSC over generalized fading channels with unequal received signal strengths. Chapter 4, 5 and 6 are dedicated to ABER analyses of different diversity receiver structures over Rayleigh, Nakagami-*m* and Ricean fading channels respectively. Computational and simulation results are provided to highlight the advantage of αr -SDC scheme over α -SDC and r-SDC schemes. Finally, Chapter 7 summarizes the main conclusions and provides suggestions for further work in this area.

Chapter 2

SYSTEM MODEL

Consider coherent detection of BPSK signals in slow, frequency non-selective fading channels with additive white Gaussian noise (AWGN). Suppose there are L independent diversity paths, each receiving locally coherent signals with statistically independent random amplitudes and random phase angles. This model is also equivalent to a tapped-delay-line model for a frequency selective channel with a channel length L. The low-pass equivalent of the received signal at the i-th branch before phase compensation is

$$w_i = \alpha_i e^{j\phi_i} b_0 + \eta_i \, , \; i = 1, ..., L \qquad (2\text{-}1)$$

where α_i, ϕ_i and η_i denote the fading amplitude, random fading phase uniformly distributed over $\left[-\pi \quad \pi\right]$ and additive complex Gaussian noise in the i-th branch respectively. Also, we have $b_0 \in \left\{\pm\sqrt{E_b}\right\}$ with equal a priori probability, where E_b corresponds to the energy per information bit.

The low-pass equivalent of the received signal at the i-th branch after phase compensation can be written as

$$r_i = \text{Re}\left\{w_i e^{-j\phi_i}\right\} = \alpha_i \cdot b_0 + n_i \, , \; i = 1, ..., L \qquad (2\text{-}2)$$

where $n_i = \text{Re}\left\{\eta_i e^{-j\phi_i}\right\}$ is assumed to be i.i.d with zero mean and variance $E\left[n_i^2\right] = N_0/2 = \sigma^2 \, , i = 1, \cdots, L$. In the following, we will define the instantaneous SNR for the i-th path as $\gamma_i = \alpha_i^2 E_b / N_0$. The corresponding average SNR for the i-th path is given by $\overline{\gamma}_i = \Omega_i E_b / N_0$. Also, notations $\overline{\gamma}_b = L \cdot E_b / N_0$ and $\overline{\gamma}_c = E_b / N_0$ denote the average SNR/bit and average SNR/bit/branch respectively.

With respect to Figure 2.1, the predetection diversity combiner signal output is given by

$$Z = \sum_{i=1}^{L} g_i w_i \qquad (2\text{-}3)$$

where the signal plus noise (i.e., matched filter output) in each branch is multiplied by a voltage gain factor g_i and then added in a linear combiner with the similar signals from other branches. The values of the gain factors depend on the type of combining that is desired, and they are summarized bellows:

MRC: $g_i = \alpha_i \exp\left(-j\phi_i\right)$

EGC: $g_i = \exp\left(-j\phi_i\right)$

SDC: $g_i = \begin{cases} \exp\left(-j\phi_i\right) & i = k \\ 0 & i \neq k \end{cases}$

The values of the gain factors depend on the type of combining that is desired, and they are summarized below:

$$k = \begin{cases} \arg\max\left|\alpha_i r_i\right| & \alpha r - SDC \\ \arg\max\left|r_i\right| & r - SDC \\ \arg\max \alpha_i & \alpha - SDC \\ \arg\max\left|\alpha_i w_i\right| & \alpha w - SDC \end{cases}$$

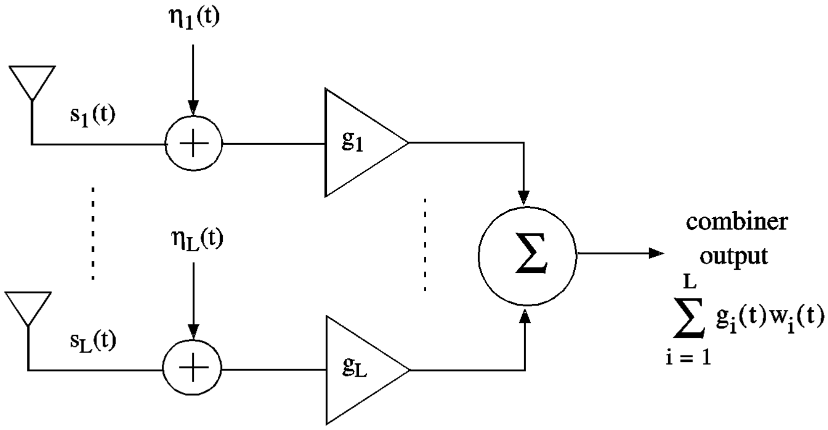

$$s_i(t) = \sqrt{E_b}\alpha_i(t)\exp[j\phi(t)]\exp[j(2\pi f_c t + \theta_m(t))]$$

$$w_i(t) = \sqrt{E_b}\alpha_i(t)\exp[j(\phi(t) + \theta_m(t))] + \eta_i(t)$$

f_c	carrier frequency
$\alpha_i(t)$	random fading amplitude process
$\phi_i(t)$	uniformly distributed random phase process
$\eta_i(t)$	additive white Gaussian noise component
$\theta_m(t)$	desired phase modulation
E_b	energy per information bit

Figure 2.1 Predetection diversity systems

2.1 Fading Channel Characterization and Modeling

Radio-wave propagation through wireless channels is a complicated phenomenon characterized by various effects, such as multipath and shadowing. A precise mathematical description of this phenomenon is either unknown or too complex for tractable communication systems analyses. However, considerable efforts have been devoted to the statistical modeling and characterization of these different effects. The result is a range of relatively simple and accurate statistical models for fading channels which depend on the particular propagation environment and the underlying communication scenario.

When a received signal experiences fading during transmission, both its envelope and phase fluctuate over time. For coherent modulations, the fading effects on the phase can severely degrade performance unless measures are taken to compensate for them at the receiver. Most often, analyses of systems employing such modulations assume that phase effects due to fading are perfectly corrected at the receiver, resulting in what is referred to as coherent demodulation. For non-coherent detection, phase information is not needed at the receiver and therefore the phase variation due to fading does not affect the performance. Hence performance analyses for both coherent and non-coherent detection over fading channels requires only knowledge of the fading envelope statistics. We will first review some basics of the fading channels.

2.1.1 Flat and Frequency Selective Fading

Frequency selectivity is an important characteristic of fading channels. If all the spectral components of the transmitted signal are affected in a similar manner, the fading is said to be flat. This is the case for narrowband systems in which the transmitted signal bandwidth is much smaller than the channel's coherent bandwidth f_c. This bandwidth measures the frequency range over which the fading process is correlated and is defined as the frequency bandwidth over which the correlation function of two samples of the channel response taken at the same time but at different frequencies falls below a suitable value. In addition, the coherence bandwidth is related to the maximum delay spread $\tau_{\max}$ by

$$f_c = \frac{1}{\tau_{\max}} \tag{2-4}$$

On the other hand, if the spectral components of the transmitted signal are affected by different amplitude gains and phase shifts, the fading is said to be frequency selective. This applies to wideband systems in which the transmitted bandwidth is larger than the channel's coherence bandwidth.

2.1.2 Slow and Fast Fading

The distinction between slow and fast fading is important for the mathematical modeling of fading channels and for the performance evaluation of communication systems operating over these channels. This notion is related to the coherence time T_c of the channel, which measures the period of time over which the fading process is correlated (or equivalently, the period of time after which the correlation function of two samples of the channel response taken at the same frequency but different time instants drops below a certain predetermined threshold). The coherence time is closely related to Doppler spread f_d by

$$T_c \approx \frac{1}{f_d} \tag{2-5}$$

The fading is said to be slow if the symbol time duration T_s is smaller than the channel's coherence time T_C, that is, the channel changes much slower than symbol duration. This does not imply that the effects of the channel can be neglected but it is possible to track the changes in the channel to appropriately compensate for the channel dynamics.

Fast fading, on the other hand, occurs when the channel varies rapidly. This causes frequency dispersion due to Doppler spreading, which leads to signal distortion. In practice, since the relationship between symbol time duration and Doppler spread, fast fading only occurs for very low data rates.

2.2 Statistical Channel Models

Multipath fading is due to the constructive and destructive combination of randomly delayed, reflected, scattered and diffracted signal components. This type of fading is relatively fast and is therefore responsible for the short term signal variations. Depending on the nature of the radio propagation environment, there are different models describing the statistical behavior of the multipath fading envelope.

2.2.1 Rayleigh Fading Model

The Rayleigh distribution is frequently used to model multipath fading with no direct line-of-sight (LOS) path. In this case, the probability density function (PDF) of fading amplitude of *i*-th path α_i is given by

$$f_{\alpha_i}\left(\alpha_i\right) = \frac{2\alpha_i}{\Omega_i}\exp\left(-\frac{\alpha_i^2}{\Omega_i}\right), \alpha_i \geq 0 \tag{2-6}$$

where $\Omega_i = E\left[\alpha_i^2\right]$ and $E\left[\cdot\right]$denotes the expectation of its argument. We define the instantaneous and mean of SNR of the *i*-th path as $\gamma_i = \alpha_i^2 E_b / N_0$ and $\overline{\gamma}_i = \Omega_i E_b / N_0$, the PDF of γ_i can be obtained as

$$f_{\gamma_i}\left(\gamma_i\right) = \frac{1}{\overline{\gamma}_i}\exp\left(-\frac{\gamma_i}{\overline{\gamma}_i}\right) \tag{2-7}$$

Consequently, the cumulative distribution function (CDF) of γ_i is readily shown as

$$F_{\gamma_i}\left(\gamma_i\right) = 1 - \exp\left(-\frac{\gamma_i}{\overline{\gamma}_i}\right) \tag{2-8}$$

Also, the moment generating function (MGF) of γ_i is given by

$$\begin{aligned} \phi_{\gamma_i}\left(s\right) &= \int_0^\infty \exp\left(-s\gamma_i\right) f_{\gamma_i}\left(\gamma_i\right) d\gamma_i \\ &= \frac{1}{1+s\overline{\gamma}_i} \end{aligned} \tag{2-9}$$

2.2.2 Ricean Fading Model

Ricean distribution is often used to model propagation paths consisting of one strong direct LOS component and many random weaker components. The channel fading amplitude of *i*-th path α_i follows the non-central chi-square distribution

$$f_{\alpha_i}\left(\alpha_i\right) = \frac{2\left(1+K_i\right)\alpha_i}{\Omega_i}\exp\left(-K_i\right)\exp\left(-\frac{\left(1+K_i\right)\alpha_i^2}{\Omega_i}\right) I_0\left(2\alpha_i\sqrt{\frac{K_i\left(1+K_i\right)}{\Omega_i}}\right), \alpha_i \ge 0 \tag{2-10}$$

The PDF and CDF of instantaneous SNR γ_i are given by (2-11) and (2-12) respectively:

$$f_{\gamma_i}\left(\gamma_i\right) = \frac{1+K_i}{\overline{\gamma}_i}\exp\left(-K_i - \frac{1+K_i}{\overline{\gamma}_i}\gamma_i\right) I_0\left(2\sqrt{\frac{K_i\left(K_i+1\right)\gamma_i}{\overline{\gamma}_i}}\right) \tag{2-11}$$

$$F_{\gamma_i}\left(\gamma_i\right) = 1 - Q\left(\sqrt{2K_i}, \sqrt{\frac{2\left(K_i+1\right)\gamma_i}{\overline{\gamma}_i}}\right) \tag{2-12}$$

where K_i denotes the Ricean factor, $\Omega_i = E\left[\alpha_i^2\right]$, $I_0(\cdot)$ is the zero-order modified Bessel function of the first kind, which may be represented by the infinite series

$$I_0(x) = \sum_{k=0}^{\infty} \frac{(x/2)^{2k}}{k!\Gamma(k+1)}, \quad x \geq 0 \tag{2-13}$$

$\Gamma(\cdot)$ is the Gamma function, defined as

$$\Gamma(x) = \int_0^{\infty} t^{x-1} e^{-t} dt, \quad x \geq 0 \tag{2-14}$$

and the first-order Marcum Q-function $Q(.,.)$ is defined as

$$Q(a,b) = \int_b^{\infty} x \exp\left(-\frac{x^2 + a^2}{2}\right) I_0(ax)\, dx \tag{2-15}$$

Taking the Laplace transform of (2-11), we obtain the MGF of γ_i as

$$\phi_{\gamma_i}(s) = \frac{1+K_i}{1+K_i+s\overline{\gamma}_i} \exp\left(-\frac{sK_i\overline{\gamma}_i}{1+K_i+s\overline{\gamma}_i}\right) \tag{2-16}$$

Figure 2.2 illustrates the Ricean PDF for $\Omega = 1$ and various values of the Ricean factor *K*. Note that the tail of the Ricean PDF diminishes as Ricean factor *K* increases. This means that it is less likely to have large variations on the fading amplitude for the large *K* values.

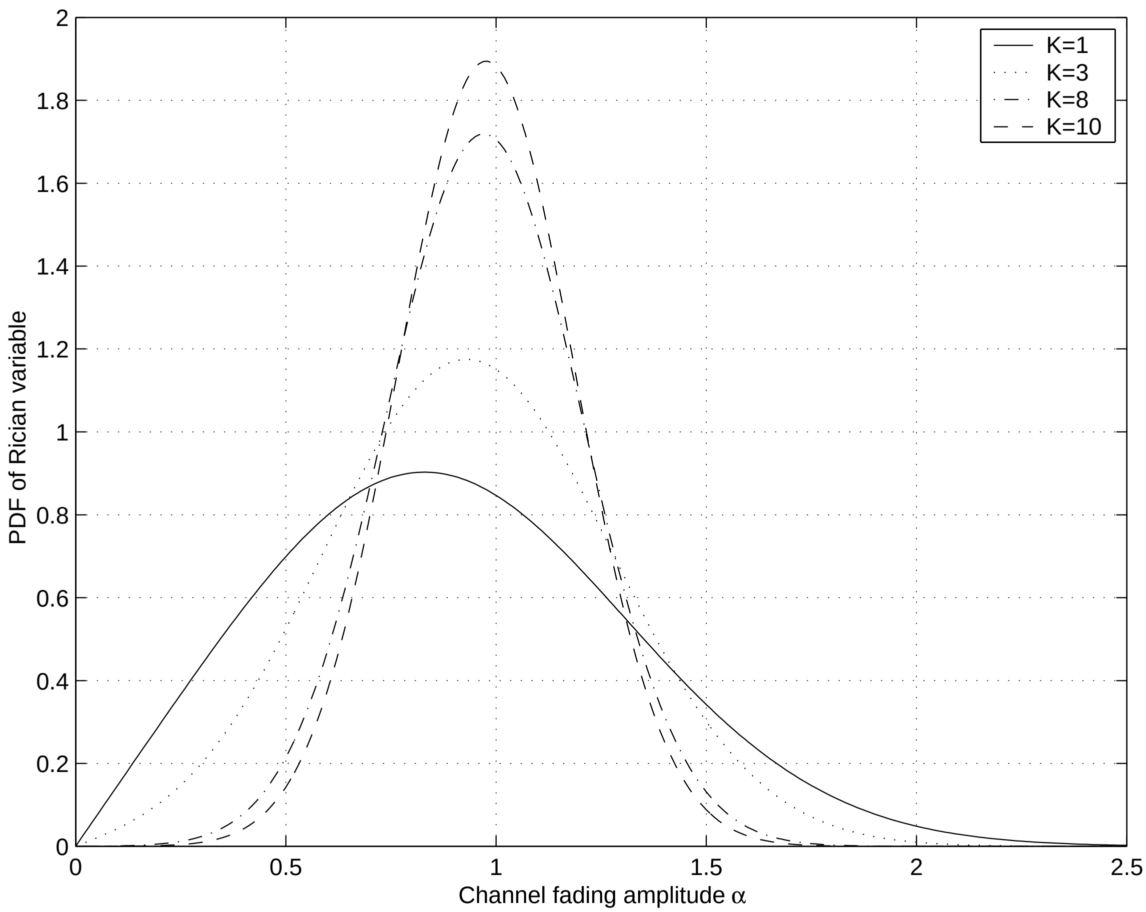

Figure 2.2 Normalized Ricean PDF for various *K* values.

2.2.3 Nakagami-*m* Fading Model

The Nakagami-*m* distribution is the widely accepted statistical fading model due to both its good fit with experimental results and its versatility. It covers a wide range of fading scenarios by varying its fading severity index *m*. The model also includes the Rayleigh ($m=1$) and one-sided Gaussian ($m=1/2$) distribution as special cases, and closely approximates the Ricean distribution via relationship $m=(K+1)^2/(2K+1)$.

The Nakagami-*m* PDF is in essence a central chi-square distribution given by [20]

$$f_{\alpha_i}(\alpha_i)=\frac{2m_i^{m_i}\alpha_i^{2m_i-1}}{\Gamma(m_i)\Omega_i^{m_i}}\exp\left(-\frac{m_i\alpha_i^2}{\Omega_i}\right),\quad \alpha_i\geq 0 \tag{2-17}$$

Hence, the PDF and CDF of instantaneous SNR will take the form of (2-18) and (2-19) respectively:

$$f_{\gamma_i}(\gamma_i) = \frac{1}{\Gamma(m_i)} \left(\frac{m_i}{\overline{\gamma}_i} \right)^{m_i} \gamma_i^{m_i - 1} \exp\left(-\frac{m_i \gamma_i}{\overline{\gamma}_i} \right) \tag{2-18}$$

$$F_{\gamma_i}(\gamma_i) = \frac{\gamma\left(m_i, \gamma_i m_i / \overline{\gamma}_i\right)}{\Gamma(m_i)} \tag{2-19}$$

where $\Omega_i = E\left[\alpha_i^2\right]$, $m_i = \Omega_i^2 \Big/ E\left[\left(\alpha_i^2 - \Omega_i^2\right)\right] \geq 0.5$ denotes the fading severity index of the *i*-th path and the incomplete Gamma function $\gamma(.,.)$ is defined as

$$\gamma(a, x) = \int_0^x t^{a-1} \exp(-t)\, dt \tag{2-20}$$

The MGF of γ_i is given by

$$\phi_{\gamma_i}(s) = \left(\frac{m_i}{m_i + s\overline{\gamma}_i} \right)^{m_i} \tag{2-21}$$

Figure 2.3 depicts the Nakagami-*m* PDF for $\Omega = 1$ and various values of the fading severity index *m*. Once again, it is observed that when fading severity index *m* increases, large fluctuations of fading amplitudes are less likely.

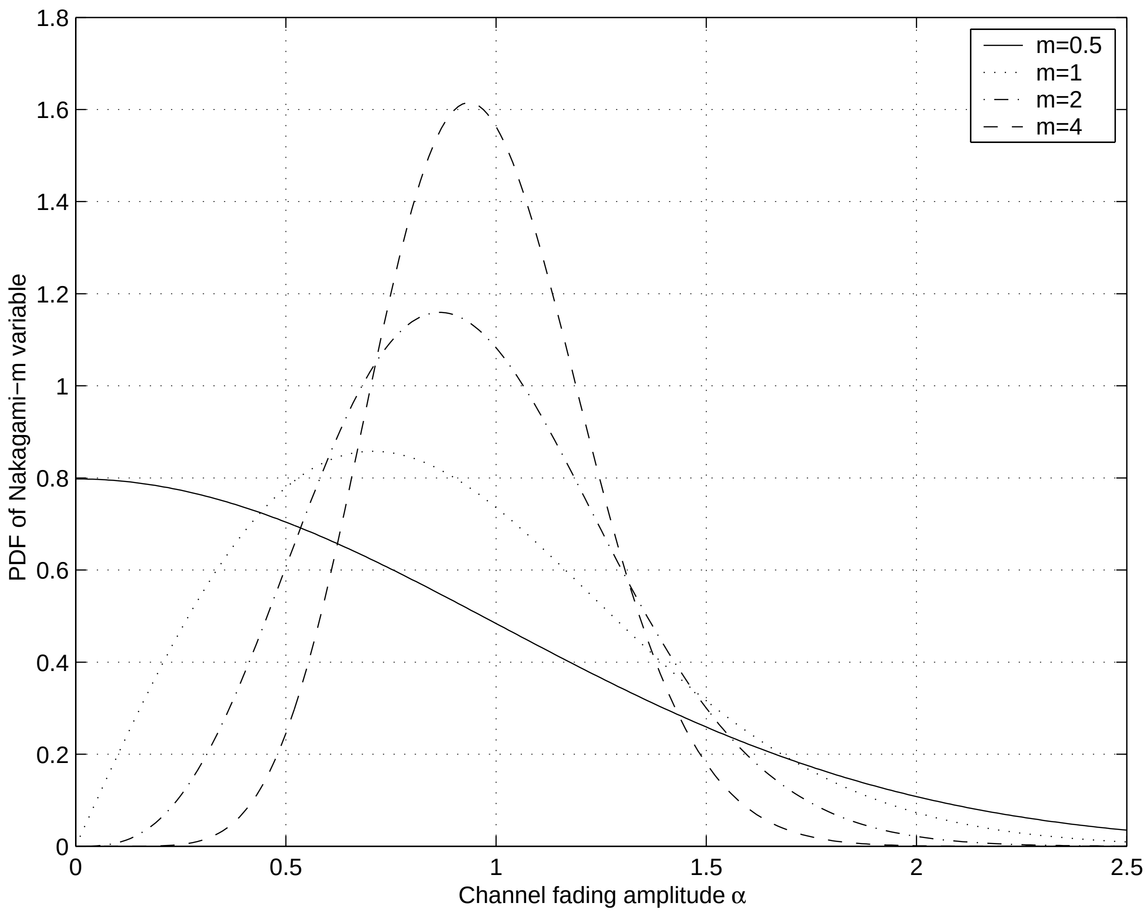

Figure 2.3 Nakagami-*m* PDF for $\Omega = 1$ and various values of the fading severity index *m*.

Chapter 3

ERROR PROBABILITY ANALYSIS OF DIVERSITY SYSTEMS

Our repetitive use of the word performance thus far brings us to the fundamental questions: “what type of measures of performance is applicable to practical communication system design?”. The clarification of this question will help us to gain insights of the advantages and disadvantages of different modulation/diversity schemes over fading channels.

3.1 Performance Criterion

Probably the most common and best understood performance metric of a digital communication system is the average SNR. Most often, this is measured at the output of the receiver and is thus related directly to the data detection itself. Of the several possible performance measures that exist, it is typically the easiest to evaluate and most often serves as an excellent indicator of the overall fidelity of the system. Although, traditionally, the term *noise* in signal-to-noise ratio refers to the ever-present thermal noise at the input to the receiver, in the context of a communication system subject to fading impairment, the more appropriate performance metric is average SNR, where the word average refers to statistical averaging over the probability distribution of the fading. In simple mathematical terms, if γ_i denotes the instantaneous SNR (a random variable) at the diversity combiner output, then

$$\overline{\gamma} = \int_0^\infty \gamma f_\gamma(\gamma)\, d\gamma \tag{3-1}$$

where $f_\gamma(\cdot)$ denotes the PDF of γ. We can rewire the (3-1) in terms of the MGF associated with γ, namely,

$$\phi_\gamma(s) = \int_0^\infty f_\gamma(\gamma) e^{-s\gamma}\, d\gamma \tag{3-2}$$

Taking the derivative of (3-2) with respect to s and evaluating the resulting expression at $s=0$, we see immediately that

$$\bar{\gamma} = \left. \frac{d\phi_{\gamma}(s)}{ds} \right|_{s=0} \tag{3-3}$$

In other words, the ability to evaluate the MGF of the instantaneous SNR allows immediate evaluation of the average SNR via a simple mathematical operation: differentiation.

The second performance criterion is the average bit error rate. This metric can be evaluated by averaging the conditional error probability (CEP) over the PDF of combiner output SNR. Suppose the CEP is of the form

$$P_b(\gamma) = a\,\mathrm{erfc}\left(\sqrt{b\gamma}\right) \tag{3-4}$$

such as would be the case for coherent detection of PSK signals or coherent detection of orthogonal FSK signals. Then, the ABER can be written as

$$P_b = \int_0^{\infty} P_b(\gamma)\, f_{\gamma}(\gamma) d\gamma \tag{3-5}$$

3.2 Generic Formulas for the Average Bit Error Rate

In this section, we derive analytical expressions for computing the ABER of BPSK signals for different receiver structures over generic fading channels (i.e., Rayleigh, Nakagami-*m* and Ricean). The diversity receiver structures considered here are αr-SDC, α-SDC, α-GSC, *r*-SDC and MRC. Note that the development of subsequent ABER expressions are based on assumption that the diversity paths are independent but non-identically distributed (i.n.d).

3.2.1 ABER for αr-SDC

The LLR for binary antipodal signaling in the *i*-th branch is given by the product of fading amplitude and output of matched filter, viz.,

$$\begin{aligned}\Lambda_i &= \ln \frac{f_w\left(w_i \middle| \alpha_i, \phi_i, b_0 = \sqrt{E_b}\right)}{f_w\left(w_i \middle| \alpha_i, \phi_i, b_0 = -\sqrt{E_b}\right)} \\ &= \ln \frac{\exp\left(-\left|w_i - \alpha_i e^{j\phi_i}\sqrt{E_b}\right|^2 \middle/ N_0\right)}{\exp\left(-\left|w_i + \alpha_i e^{j\phi_i}\sqrt{E_b}\right|^2 \middle/ N_0\right)} \\ &= \frac{4\sqrt{E_b}}{N_0}\alpha_i r_i\end{aligned} \tag{3-6}$$

where $f_w(\cdot)$ corresponds to the Gaussian density function. Without loss of generality, we assume that $\sqrt{E_b}$ was transmitted, Hence, the ABER of BPSK in conjunction with αr-SDC receiver operating over a generic fading channel with i.n.d diversity paths is given by

$$\begin{aligned}P_b &= \sum_{i=1}^{L} \Pr\left(r_i < 0 \mid b_0 = \sqrt{E_b}, \left|\alpha_i r_i\right| > \left|\alpha_j r_j\right|, \forall j \neq i\right) \\ &= \sum_{i=1}^{L} \Pr\left(\alpha_i r_i + \max_{j, j \neq i}\left\{\left|\alpha_j r_j\right|\right\} < 0\right) \\ &= \sum_{i=1}^{L} \Pr\left(Z_i < 0\right)\end{aligned} \tag{3-7}$$

where $Z_i = R_i + \alpha_i r_i$ and $R_i = \max_{j, j \neq i}\left\{\left|\alpha_j r_j\right|\right\}$.

Since $R_i > 0$ and is independent with $\alpha_i r_i$, (3-7) can be rewritten as

$$\begin{aligned}P_b &= \sum_{i=1}^{L} \int_{-\infty}^{\infty} \Pr\left(R_i \leq -x \mid \alpha_i r_i = x\right) f_{\alpha_i r_i}(x)\, dx \\ &= \sum_{i=1}^{L} \int_{-\infty}^{0} F_{R_i}(-x) f_{\alpha_i r_i}(x)\, dx\end{aligned} \tag{3-8}$$

where $f_{\alpha_i r_i}(\cdot)$ denotes the PDF of random variable $\alpha_i r_i$ and $F_{R_i}(\cdot)$ denotes the CDF of R_i. Since $|\alpha_i r_i|$'s are independent, the CDF of R_i is simply the product of the CDFs of $|\alpha_i r_i|$, namely, $F_{R_i}(x) = \prod_{j=1, j\neq i}^{L} F_{|\alpha_i r_i|}(x)$. Hence, (3-8) can be rewritten as

$$P_b = \sum_{i=1}^{L} \int_0^{\infty} \left(\prod_{j=1, j\neq i}^{L} F_{|\alpha_j r_j|}(x) \right) f_{\alpha_i r_i}(-x)\, dx \tag{3-9}$$

where $F_{|\alpha_i r_i|}(\cdot)$ is defined as

$$F_{|\alpha_i r_i|}(x) = \int_{-x}^{x} f_{\alpha_i r_i}(y)\, dy \tag{3-10}$$

In order to compute the ABER described in (3-9), a numerical integration method can be applied. It is apparent that the knowledge of $f_{\alpha_i r_i}(\cdot)$ and $F_{|\alpha_i r_i|}(\cdot)$ is further needed for computing the ABER. Fortunately, the PDF of $\alpha_i r_i$ can be obtained for Rayleigh, Nakagami-*m* and Ricean fading channels. The derivation of PDF of $\alpha_i r_i$ will be treated in the following chapters. Once we have PDF of $\alpha_i r_i$, the CDF of $|\alpha_i r_i|$ is simply the integration of PDF of $\alpha_i r_i$ defined by (3-10).

In [19], the authors have also suggested a suboptimal selection rule αw-SDC which does not require phase compensation in the selection process. It is obvious that αw-SDC will be inferior to αr-SDC since $|\alpha_i r_i| = \left|\alpha_i \operatorname{Re}\left\{w_i e^{-j\phi_i}\right\}\right|$ compensates for the random phase before selecting the path with the largest magnitude of the LLR. We will examine the efficacy of αw-SDC receiver with dissimilar received mean signal strengths via simulation technique owing to the difficulty in deriving an analytical expression for computing the ABER of this selection rule.

3.2.2 ABER for α - SDC and α -GSC

The ABER for receiver that employs α-SDC in conjunction with coherent detection of BPSK signaling is given by [18]

$$P_b = \sum_{i=1}^{L} \Pr\left(r_i < 0 \mid b_0 = \sqrt{E_b}, \gamma_i > \gamma_j, \forall j \neq i \right)$$
$$= \sum_{i=1}^{L} \int_0^{\infty} \frac{1}{2} \operatorname{erfc}\left(\sqrt{\gamma_i} \right) f_{\gamma_i}(\gamma_i) \prod_{j=1, j\neq i}^{L} F_{\gamma_j}(\gamma_i) d\gamma_i \tag{3-11}$$

where $f_{\gamma_i}(.)$ and $F_{\gamma_i}(\cdot)$ are PDF and CDF of instantaneous SNR of *i*-th path.

It is also advantageous to compare the error rate performance of αr-SDC with a generalized selection combining scheme α-GSC (*N, L*), where *N* paths with the largest SNRs are selected and combined in a similar fashion to MRC. For coherent detection of BPSK signals, the expression of ABER for α-GSC (*N, L*) receiver over fading channels with i.n.d diversity paths is given by [23]:

$$P_b = \Pr\left(\sum_{i=1}^{N} \alpha_{(i)} r_{(i)} < 0 \mid b_0 = \sqrt{E_b}, \infty > \gamma_{(1)} > \gamma_{(2)} > \cdots > \gamma_{(L)} > 0 \right)$$
$$= \frac{1}{\pi} \int_0^{\pi/2} \phi_{\gamma_{gsc}}\left(\frac{1}{\sin^2\theta} \right) d\theta \tag{3-12}$$

where $\gamma_{(i)}$'s denote the ordered random variables of γ_i in descending order, $\gamma_{gsc} = \sum_{i=1}^{N} \gamma_{(i)}$ is the GSC combiner output SNR with N rake fingers, $\phi_{\gamma_{gsc}}(.)$ corresponds to the moment generating function of the combiner's output SNR. Recognizing that $\phi_{\gamma_{gsc}}(.)$ is the key to unified analysis of α-GSC(*N,L*) receiver over generalized fading channel, the neat solution is given in [28]:

$$\phi_{\gamma_{gsc}}(s) = \sum_{\zeta \in T_{L,N}} \int_0^{\infty} e^{-sx} f_{\zeta(L-N+1)}(x) \left[\prod_{i=1}^{L-N} F_{\zeta(i)}(x) \right] \left[\prod_{k=L-N+2}^{L} \phi_{\zeta(k)}(s,x) \right] dx, 1 \le N \le L \tag{3-13}$$

where $f_i(.)$ and $F_i(.)$ are PDF and CDF of the instantaneous SNR γ_i of *i*-th path respectively and $\phi_i(s,x)$ denotes the marginal MGF of γ_i which is defined as

$$\phi_i(s,x) = \int_x^{\infty} e^{-st} f_i(t)\, dt \tag{3-14}$$

Notation $\zeta \in T_{L,N} \triangleq \zeta \in S_L, \zeta(1) < \zeta(2) < \cdots < \zeta(L-N), \zeta(L-N+2) < \cdots < \zeta(L)$, S_L is the set of all permutations of integers $\{1,2,\cdots,L\}$ and $\zeta \in S_L$ denotes the specific function $\zeta = (\zeta(1), \zeta(2), \cdots, \zeta(L))$ which permutes the integers $\{1,2,\cdots,L\}$. The construction of S_L can be implemented within a few command lines in MATLAB.

3.2.3 ABER for *r*-SDC

In [18], an analytical framework for studying the efficacy of *r*-SDC over fading channels is developed. The ABER of BPSK is given by

$$\begin{aligned} P_b &= 1 - \sum_{i=1}^{L} \Pr\left(r_i > 0 \mid b_0 = \sqrt{E_b}, |r_i| > |r_j|, \forall j \neq i \right) \\ &= 1 - \sum_{i=1}^{L} \int_0^\infty g(z_i) \prod_{j=1, j\neq i}^{L} \left[\int_{-z_i}^{z_i} g(z_j)\, dz_j \right] dz_i \end{aligned} \tag{3-15}$$

where $z_i = r_i \big/ \sqrt{N_0/2}$, it is apparent that only the knowledge of the PDF of random variable of z_i is further required. Since $z_i = \dfrac{\alpha_i b_0 + n_i}{\sqrt{N_0/2}}$ (assume $b_0 = \sqrt{E_b}$ was transmitted without loss of generality), it is evident that the PDF of z_i is simply the convolution of the PDF of fading amplitude α_i and the PDF of real Gaussian noise n_i.

3.2.4 ABER for MRC

The SNR at the output of a MRC combiner is given by

$$\gamma = \sum_{i=1}^{L} \gamma_i = \sum_{i=1}^{L} \frac{\alpha_i^2 E_b}{N_0} \tag{3-16}$$

Using the alternate representation of the Gaussian *Q*-function, viz.,

$$Q(x) = \frac{1}{\pi} \int_0^{\pi/2} \exp\left(-\frac{x^2}{2\sin^2\theta} \right) d\theta \tag{3-17}$$

it is straight-forward to show that the ABER for BPSK with coherent MRC receiver is given by

$$P_b = \frac{1}{\pi}\int_0^{\pi/2}\prod_{i=1}^{L}\phi_{\gamma_i}\left(\frac{1}{\sin^2\theta}\right)d\theta \qquad (3\text{-}18)$$

where $\phi_{\gamma_i}(\cdot)$ denotes MGF of SNR of the *i*-th path.

3.3 Implementation Complexity

Since the improvements achieved through more sophisticated diversity combining methods are usually at the expense of increased receiver complexity, it is instructive to compare all of the above mentioned diversity combining methods in terms of computational delay and hardware complexity.

For selection diversity, the sign of the matched filter output of selected branch represents the hard decision rule (i.e., decide that $\sqrt{E_b}$ was transmitted if $r_k > 0$, and decide that $-\sqrt{E_b}$ was transmitted if $r_k < 0$) while the magnitude of α_k, r_k, $\alpha_k w_k$ and $\alpha_k r_k$ provide the reliability of the hard decision for α-SDC, *r*-SDC, αw-SDC and αr-SDC respectively. Moreover, α-SDC and αw-SDC do not require phase information $\phi_i\,(i = 1,\cdots,L)$ in the selection process. Since α-SDC and αw-SDC require phase compensation only in the selected branch, their hardware complexities are simpler than αr-SDC and MRC receiver implementations.

Assuming an M_1-level quantization (or $\log_2(M_1)$ bits) for α_i and M_2-level quantization (or $\log_2(M_2)$ bits) for r_i, the required register sizes for storing the decision statistics $X = \sum_{i=1}^{N}\alpha_{(i)}r_i$ for α-GSC(*N*,*L*) is $\lceil \log_2 N + \log_2 M_1 + \log_2 M_2 \rceil$ bits for $2 \le N \le L$. Whereas, the register size requirements for αr-SDC (or αw-SDC), *r*-SDC and α-SDC are $\lceil \log_2 M_1 + \log_2 M_2 \rceil$, $\lceil \log_2 M_2 \rceil$ and $\lceil \log_2 M_1 \rceil$ bits respectively.

Also, the α-GSC (*N, L*) involves $L-1$ comparisons and $N-1$ summations. The αr-SDC, αw-SDC and *r*-SDC schemes require $L-1$ comparisons (subtractions) and reading only the sign bit after each subtraction. Therefore, the α-GSC (*N, L*) (which includes MRC for $N = L$) incurs a larger computational delay and hardware complexity than αr-SDC, αw-SDC and *r*-SDC schemes. Moreover, we will soon observe (from figure 4.3) that αw-SDC and αr-SDC yield performance comparable to α-GSC(2,6) and α-GSC(3,6) respectively, in a UMTS Vehicular A channel model and Rayleigh fading. As such, the low-complexity αw-SDC and αr-SDC receiver structures represent a viable alternative for rake receiver designs that currently employ α-GSC(*N,L*) selection rule.

Chapter 4

DIVERSITY RECEIVER PERFORMANCE OVER RAYLEIGH FADING CHANNELS

In Chapter 3, we presented generic expressions for computing the ABER of αr-SDC, α-SDC, α-GSC, r-SDC and MRC over generalized i.n.d fading channels. In this chapter, we are interested in the theoretical performance analysis and comparative study of different diversity combining schemes over Rayleigh fading channels. Both computational and simulations results are presented to highlight performance improvements with αr-SDC and αw-SDC schemes over α-SDC and r-SDC methods.

4.1 Performance Analysis over Rayleigh Fading

In this section, analytical expressions for computing the ABER for different receiver structures over Rayleigh fading channels with i.n.d diversity paths are detailed, based on the generic formula presented in Chapter 3.

- αr-SDC

Since $\alpha_i r_i = \alpha_i^2 \cdot \sqrt{E_b} + \alpha_i n_i$, the PDF of $\alpha_i r_i$ can be obtained through convolution of Gaussian and Rayleigh PDFs, viz.,

$$\begin{aligned} f_{\alpha_i r_i}(x) &= \int_0^\infty \frac{1}{\sqrt{2\pi\alpha_i^2 N_0/2}} \exp\left(-\frac{\left(x-\alpha_i^2\sqrt{E_b}\right)^2}{\alpha_i^2 N_0}\right) \frac{2\alpha}{\Omega_i} \exp\left(-\frac{\alpha_i^2}{\Omega_i}\right) d\alpha_i \\ &= \frac{1}{\Omega_i}\sqrt{\frac{\Omega_i}{E_b\Omega_i + N_0}} \exp\left(\frac{2x\sqrt{E_b} - 2|x|\sqrt{\left(E_b\Omega_i + N_0\right)/\Omega_i}}{N_0}\right) \end{aligned} \tag{4-1}$$

with the aid of identity [21, eq. 3.325]:

$$\int_0^\infty \exp\left(-px^2 - \frac{q}{x^2}\right) dx = \frac{1}{2}\sqrt{\frac{\pi}{p}} \exp\left(-2\sqrt{pq}\right) \qquad p>0, q>0 \tag{4-2}$$

From the definition of $F_{|\alpha_i r_i|}(\cdot)$, we also have

$$F_{|\alpha_i r_i|}(x) = \frac{1}{\Omega_i}\sqrt{\frac{\Omega_i}{E_b\Omega_i + N_0}}\left[\frac{1}{a_i}\left(1-e^{-a_i x}\right)+\frac{1}{b_i}\left(1-e^{-b_i x}\right)\right] \tag{4-3}$$

where

$$a_i = \frac{2\sqrt{E_b} + 2\sqrt{\left(E_b\Omega_i + N_0\right)/\Omega_i}}{N_0}$$
$$b_i = \frac{-2\sqrt{E_b} + 2\sqrt{\left(E_b\Omega_i + N_0\right)/\Omega_i}}{N_0}$$

For the special case of i.i.d Rayleigh fading, it is easy to verify that (4-1) and (4-3) reduces to [19, eq. (20)] and [19, eq. (21)] by setting $\Omega_i = 1$.

Recognizing the maximum of $|\alpha_1 r_1|$ and $|\alpha_2 r_2|$ dominates the sign of $\alpha_1 r_1 + \alpha_2 r_2$, the ABER performance of dual-diversity αr-SDC receiver is identical to the dual-diversity MRC[22], viz.,

$$P_b = \frac{1}{2}\left[\frac{\bar{\gamma}_1}{\bar{\gamma}_1-\bar{\gamma}_2}\left(1-\sqrt{\frac{\bar{\gamma}_1}{1+\bar{\gamma}_1}}\right)+\frac{\bar{\gamma}_2}{\bar{\gamma}_2-\bar{\gamma}_1}\left(1-\sqrt{\frac{\bar{\gamma}_2}{1+\bar{\gamma}_2}}\right)\right], \bar{\gamma}_1 \neq \bar{\gamma}_2 \tag{4-4}$$

- α-SDC

If we substitute PDF and CDF of SNR that correspond to Rayleigh faded signal amplitude (i.e., eqs. (2-7) and (2-8) into eq. (3-11)), the ABER for α-SDC receiver is given by

$$\begin{aligned} P_b &= \sum_{i=1}^{L}\int_0^\infty \frac{1}{2}\operatorname{erfc}\left(\sqrt{\gamma_i}\right)\frac{1}{\bar{\gamma}_i}\exp\left(-\frac{\gamma_i}{\bar{\gamma}_i}\right)\prod_{j=1, j\neq i}^{L}\left[1-\exp\left(-\frac{\gamma_i}{\bar{\gamma}_j}\right)\right]d\gamma_i \\ &= \sum_{i=1}^{L}\frac{1}{2}\left[1-\sqrt{\frac{\bar{\gamma}_i}{\bar{\gamma}_i+1}}\right]+\sum_{i=1}^{L}\sum_{j=1}^{L-1}(-1)^j \sum_{\substack{v_1+\cdots+v_L=j \\ v_{i=0}}}\frac{\bar{\gamma}_j}{2\left(\bar{\gamma}_j+\bar{\gamma}_i\sum_{k=1}^{L}v_k\right)}\left[1-\sqrt{\frac{\bar{\gamma}_i\bar{\gamma}_j}{\bar{\gamma}_i\bar{\gamma}_j+\bar{\gamma}_j+\bar{\gamma}_i\sum_{k=1}^{L}v_k}}\right] \end{aligned} \tag{4-5}$$

where $v_k \in \{0,1\}$ for all index $k = 1,\cdots,L$.

- α -GSC

In [23], the authors have observed the closed-form expression for eq. (3-12) in Rayleigh fading as

$$P_b = \sum_{\zeta \in S_L} \sum_{k=1}^{L} \frac{p_k}{\beta_k} \left(\frac{1}{2} - \frac{1}{2\sqrt{1+\beta_k}} \right) \tag{4-6}$$

where $p_k = \dfrac{\theta_0}{N!N^{L-N}} \prod_{i=1, i \neq j}^{L} \dfrac{1}{\beta_i - \beta_k}$ and the coefficients β_k 's are defined as

$$\beta_k = \begin{cases} \theta_k / k & 1 \le k \le N \\ \theta_k / N & N+1 \le k \le L \end{cases}$$

where $\theta_0 = \prod_{k=1}^{L} 1/\overline{\gamma}_k$ and $\theta_k = \sum_{i=0}^{k-1} 1/\overline{\gamma}_{\tau(L-i)}$ for $k = 1,\cdots,L$. For the special cases of MRC and α -SDC, we simply have N=L and $N = 1$ respectively.

- r-SDC

The PDF of z_i in Rayleigh fading environment can be evaluated to be

$$\begin{aligned} g(z_i) &= \int_0^\infty \frac{1}{\sqrt{2\pi}} \exp\left(-\frac{(z_i - y)^2}{2} \right) \frac{y}{\overline{\gamma}_i} \exp\left(-\frac{y^2}{2\overline{\gamma}_i} \right) dy \\ &= \frac{1}{\sqrt{2\pi}\,(m_i + \overline{\gamma}_i)} \exp\left(-\frac{z_i^2 (2+\overline{\gamma}_i)}{4(1+\overline{\gamma}_i)} \right) D_{-2}\left(-z_i \sqrt{\frac{\overline{\gamma}_i}{1+\overline{\gamma}_i}} \right) \end{aligned} \tag{4-7}$$

where parabolic cylinder function $D_{-2}(\cdot)$ in (4-7) can be computed as

$$D_{-2}(z) = \exp\left(-\frac{z^2}{4} \right) - z \exp\left(\frac{z^2}{4} \right) \sqrt{\frac{\pi}{2}}\, \mathrm{erfc}\left(\frac{z}{\sqrt{2}} \right) \tag{4-8}$$

For the special case of dual-diversity r-SDC, it is possible to express eq. (3-15) in closed-form by equivalence with the second order coherent EGC receiver. Since the maximum of $|r_1|$ and $|r_2|$ dominates the sign of $r_1 + r_2$, it is apparent that the ABER performance of the dual-diversity *r*-SDC is identical to the dual-diversity EGC [24]. Hence, we have

$$P_b = \frac{1}{2} - \frac{\sqrt{\overline{\gamma}_1\left(\overline{\gamma}_1 + 2\right)} + \sqrt{\overline{\gamma}_2\left(\overline{\gamma}_2 + 2\right)}}{2\left(\overline{\gamma}_1 + \overline{\gamma}_2 + 2\right)} \tag{4-9}$$

- MRC

Substituting (2-9) into (3-19), we have the expression for MRC receiver over Rayleigh fading channels with i.n.d diversity paths

$$P_b = \frac{1}{\pi}\int_0^{\pi/2} \prod_{i=1}^{L} \frac{\sin^2\theta}{\sin^2\theta + \overline{\gamma}_i} d\theta \tag{4-10}$$

It is possible to evaluate (4-10) in closed-form using the integral identity derived in [5]. This development is omitted here for brevity.

4.2 Effect of Branch Correlations on Diversity Receiver Performance

The aforementioned derivations are based on the assumption of independent diversity paths. However, this is not always the case in practical systems. For example, due to the small-sized hand0held terminals equipped with multiple antennas, it is important to investigate the effect of branch correlations on different diversity combining methods. Let ρ denotes power correlation coefficient between the two signal envelopes, viz.,

$$\rho = \frac{\operatorname{cov}\left(r_1^2, r_2^2\right)}{\sqrt{\operatorname{var}\left(r_1^2\right) \cdot \operatorname{var}\left(r_2^2\right)}}, 0 \le \rho < 1 \tag{4-11}$$

The analysis for αr-SDC and *r*-SDC are not easily tractable when the diversity paths are correlated except for the special case of *L*=2. This is mainly attributed to the difficulty in deriving the joint PDF of multiple correlated random variables in a simple form. Even the analysis of α-SDC in the existing literature is limited to *L*=2 for the above mentioned reason. In the following, we present analytical expressions for computing the ABER of a dual diversity BPSK in conjunction with αr-SDC, *r*-SDC and α-SDC over correlated Rayleigh fading channels.

Since the maximum of $|r_1|$ and $|r_2|$ dominates sign of $r_1 + r_2$, the ABER of BPSK that employs dual-diversity r-SDC is identical to the dual-diversity EGC performance operating in a correlated Rayleigh fading environment, viz.,[27]

$$P_b = \frac{1}{2} - \frac{\sqrt{2}}{2} \sum_{k=1}^{\infty} \rho^{k-1} (1-\rho)^{3/2} \left[\frac{\Gamma(2k)}{2^{2k-1}\Gamma(k)} \right]^2 \Big/ \left[\Gamma(k) \Gamma\left(k + \frac{1}{2}\right) \right] \times \sum_{i=1, j \neq i}^{2} \sqrt{\frac{\overline{\gamma}_j \pi}{B}} F_2\left(\frac{1}{2}; \frac{1}{2} - k, 1-k; \frac{1}{2}, \frac{3}{2}; \frac{A\overline{\gamma}_i}{B}, \frac{A\overline{\gamma}_j}{B} \right) \tag{4-12}$$

where $A = \frac{1-\rho}{2}$ and $B = 1 + A(\overline{\gamma}_1 + \overline{\gamma}_2)$. The Appell's hypergeometric function, $F_2(.;.;.;.)$, can be evaluated in closed-form as

$$F_2\left(\tfrac{1}{2}; \tfrac{1}{2} - k, 1-k; \frac{1}{2}, \frac{3}{2}; x, y \right) = \sum_{n=0}^{k-1} \frac{(1/2)_n (1-k)_n}{(3/2)_n \, n!} (1-x)^{k-n-0.5} \, y^n \sum_{m=0}^{n} \frac{(-n)_m (k)_m}{(1/2)_m \, m!} x^m$$

where $(a)_n = \Gamma(a+n)/\Gamma(a)$ is the Pochhammer symbol and

$$(-k)_n = \begin{cases} \dfrac{(-1)^n k!}{(k-n)!} & 0 \le n \le k \\ 0 & n > k \end{cases}$$

Similarly, the ABER performance of dual-diversity αr-SDC for BPSK over correlated Rayleigh fading channels can be computed as

$$P_b = \frac{1}{\pi} \int_0^{\pi/2} \phi_\gamma \left(\csc^2 \theta \right) d\theta \tag{4-13}$$

where $\phi_\gamma(.)$ is given in [20]

$$\phi_\gamma(s) = \frac{1}{1 + (\overline{\gamma}_1 + \overline{\gamma}_2) s + (1-\rho) \overline{\gamma}_1 \overline{\gamma}_2 s^2} \tag{4-14}$$

Note that (4-13) in conjunction with (4-14) is essentially the ABER of BPSK with dual-diversity MRC in a correlated Rayleigh fading channel.

For α -SDC, the ABER of BPSK is readily computed using (4-13) except that $\phi_\gamma(.)$ is given by [28]

$$\phi_\gamma(s) = \sum_{i=1, i\neq j}^{2} \frac{\left(2A_{ij}\right)^2}{\overline{\gamma}_i B_{ij}\left(1+B_{ij}\right)} \tag{4-15}$$

where

$$A_{ij} = \frac{\sqrt{\overline{\gamma}_j\left(1-\rho\right)/2}}{\overline{\gamma}_j/\overline{\gamma}_i + s\overline{\gamma}_j\left(1-\rho\right)}$$

$$B_{ij} = \frac{\sqrt{\left[s\overline{\gamma}_i\overline{\gamma}_j\left(1-\rho\right)+\overline{\gamma}_i+\overline{\gamma}_j\right]^2 - 4\rho\overline{\gamma}_i\overline{\gamma}_j}}{s\overline{\gamma}_i\overline{\gamma}_j\left(1-\rho\right)+\overline{\gamma}_j-\overline{\gamma}_i}$$

4.3 Analytical and Simulation Results

In this section, selected computational and simulation results are provided to highlight the efficacy of different receiver structures over Rayleigh fading as well as to study the impact of unequal mean received signal strengths and branch correlations across the diversity paths on the receiver performance. The accuracy of all the analytical expressions has been validated by extensive Monte-Carlo simulation runs.

In order to perform a comparative study of diversity receiver performance with independent but non-identically distributed diversity paths, it is plausible to introduce an exponentially decaying multipath intensity profile (MIP). This is because a single parameter δ (power decay factor) can introduce mean power imbalances across the diversity paths. In this case, the mean SNR of the *k*-th path is given by

$$\overline{\gamma}_k = \frac{\left(1-e^{-\delta}\right)e^{-\delta(k-1)}}{1-e^{-L\delta}}\overline{\gamma}_b \tag{4-16}$$

and the parameter δ controls the power factor. Note that for large δ, the channel is not dispersive and very little multipath diversity is obtained. However, as $\delta \to 0$, the channel becomes more dispersive and there will be L diversity paths with almost equal mean received signal strengths. As such, (4-16) can still be used to evaluate the performance of diversity receiver with i.i.d diversity paths by setting $\delta = 10^{-5}$.

Figure 4.1 depicts the ABER performance for diversity BPSK with i.i.d diversity paths. The ABER curves obtained via the simulation approach (as indicated by the figure legends) are in good agreement with those obtained from their analytical expression counterparts (as indicated by the different line styles). It is also seen from Figure 4.1 that *r*-SDC and αw-SDC yield virtually identical performance for the dual-diversity case. However, their discrepancy gets larger as the order of diversity increases. When *L*=5, αr-SDC, αw-SDC, *r*-SDC and α-SDC receivers involve a mean SNR per bit per channel penalty of 0.7 dB, 2.0 dB, 2.6 dB and 4.1 dB respectively, with respect to MRC at ABER of 10^{-4}.

Figure 4.2 illustrates the ABER performance of diversity BPSK in Rayleigh fading and *L*=8 for several δ values. We have verified the accuracy of our analytical formulas with the results obtained using the Monte-Carlo simulation method. It is apparent from this figure that αr-SDC yields comparable performance with that of the optimal linear diversity combiner as the channel becomes less dispersive (i.e., $\delta > 2$) despite *L*=8. This observation can be attributed to the following two trends: (a) the relative diversity improvement declines with increasing *L*; (b) the statistical diversity advantage is maximum when $\delta = 0$ and relative improvement decreases with increasing δ.

In Figure 4.3, we study the ABER performance of several receiver structures for BPSK in the Vehicular A UMTS WCDMA model and Rayleigh fading. The relative mean powers (i.e., normalized by the mean power of the first path) of the UMTS channel model for Vehicular A operating environment is [0 -1 -9 -10 -15 -20] (in unit decibel). Several interesting trends can be drawn from Fig. 4. Different from the i.i.d diversity paths case, the *r*-SDC does not necessarily perform better than α-SDC for a specified average SNR per bit. This trend is in agreement with the observation in [18]. We also found that αw-

SDC and αr-SDC yield performance comparable to that of α-GSC(2,6) and α-GSC(3,6) respectively. Moreover, the αr-SDC and αw-SDC are only 0.7 dB and 2.1 dB inferior to the optimal MRC respectively at the ABER of 10^{-5} for BPSK in Rayleigh fading channels. Different from *r*-SDC scheme, αw-SDC is less susceptible to the variations in the mean received signal strengths across the diversity paths. At ABER of 10^{-5}, th diversity gain of αw-SDC is greater than that of *r*-SDC and α-SDC by 1.1 dB and 2.8 dB respectively.

Figure 4.4 depicts the ABER performance of BPSK in correlated Rayleigh fading plotted as a function of average SNR/bit/branch. To generate this plot, we have assumed $L = 4$, uniform MIP and constant correlation model with power correlation coefficient ρ. When $\rho = 0.8$, αr-SDC, αw-SDC, *r*-SDC and α-SDC suffer an average SNR/bit/branch penalty of 0.4 dB, 1.56 dB, 1.65 dB and 3.3 dB compared to MRC at ABER of 5×10^{-3}. When $\rho = 0.3$, the corresponding average SNR/bit/branch penalty at the ABER of 5×10^{-3} for αr-SDC, αw-SDC, *r*-SDC and α-SDC with respect to MRC is 0.5 dB, 1.6 dB, 1.85 dB and 3.3 dB respectively. Thus, we find that the discrepancy between the αr-SDC and MRC curves, and the αw-SDC and MRC curves decreases slightly as ρ gets larger. Although αw-SDC with i.i.d paths outperforms *r*-SDC, the difference in their performance diminishes as ρ increases. This in turn suggests that αw-SDC is more vulnerable to branch correlations compared to the *r*-SDC scheme.

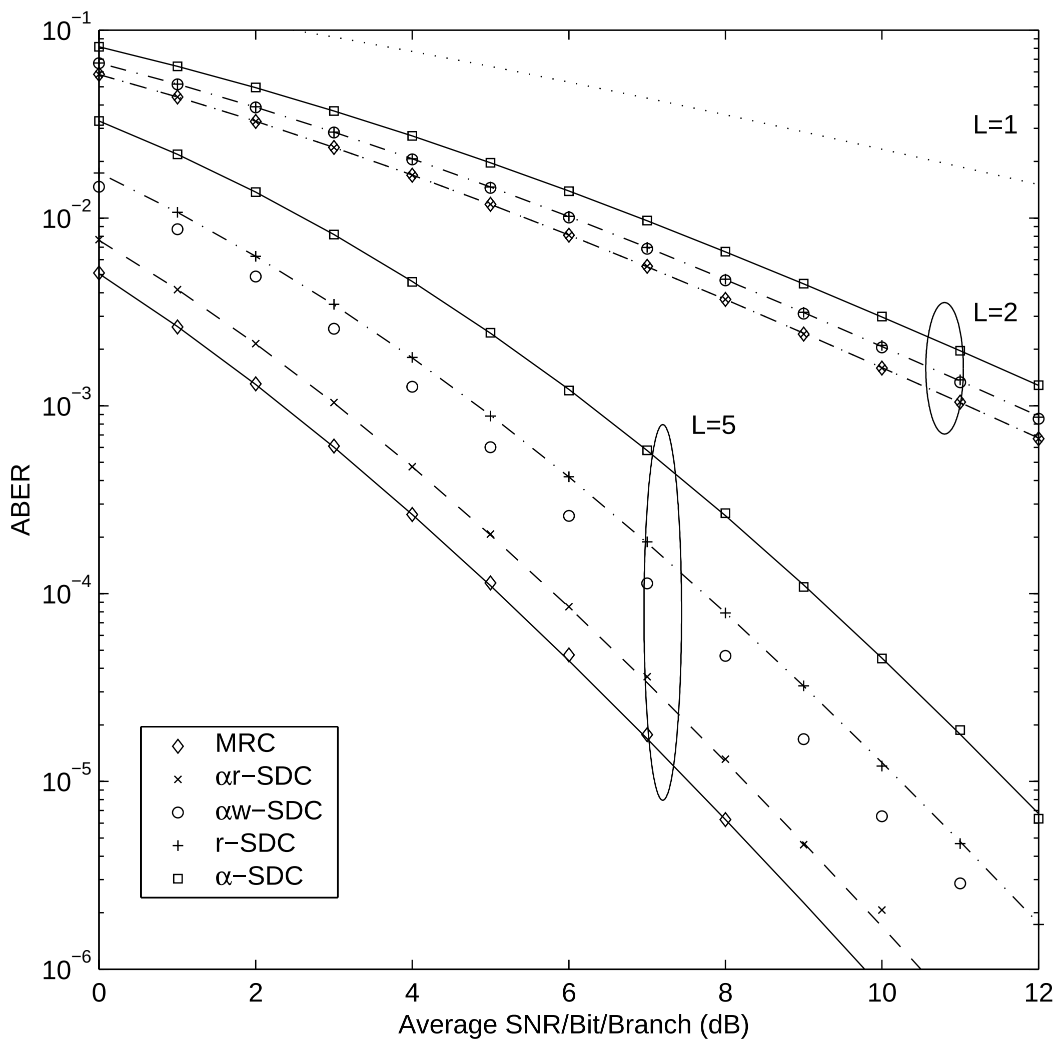

Figure 4.1 ABER performance of BPSK over i.i.d Rayleigh fading channels for different receiver structures and diversity order *L*.

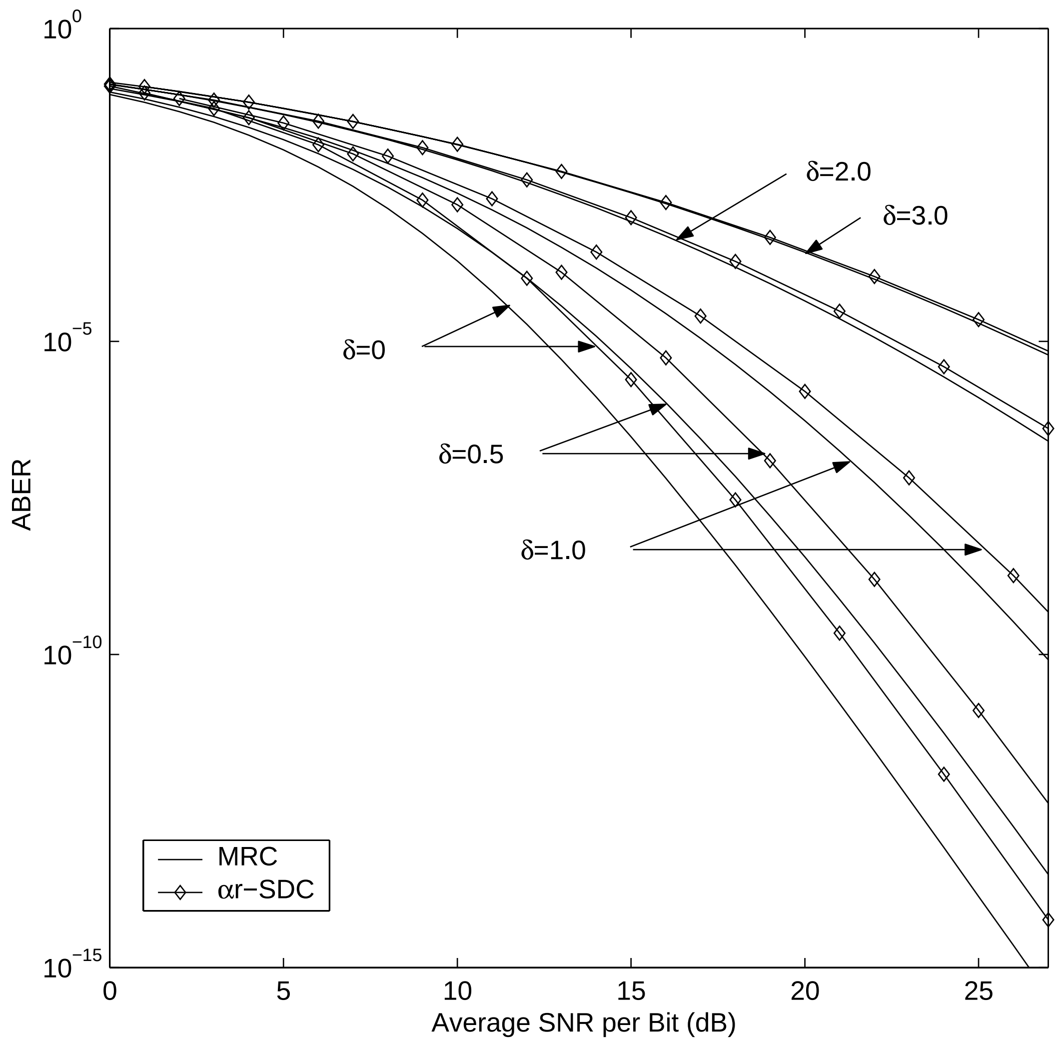

Figure 4.2 ABER of BPSK over Rayleigh fading with L=8 i.n.d diversity paths for several δ values.

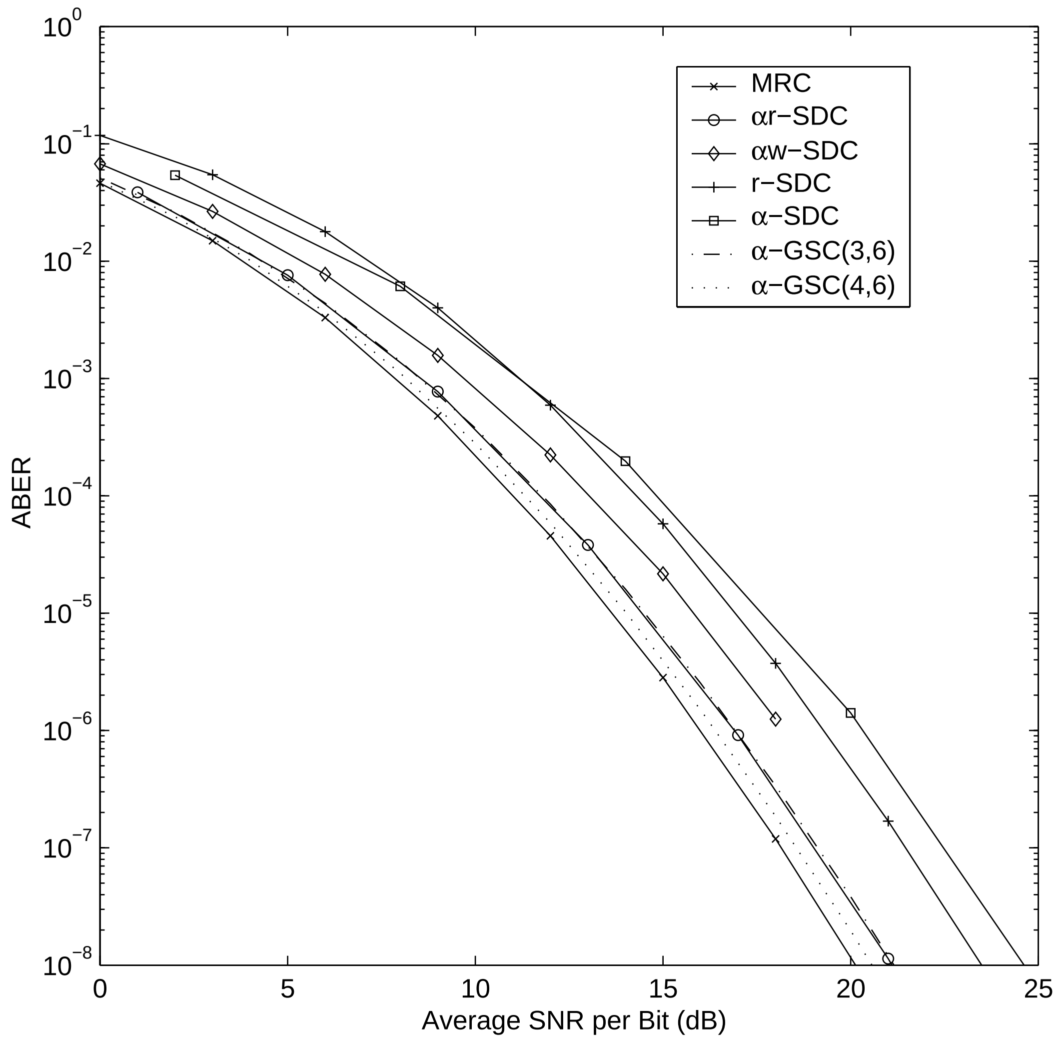

Figure 4.3 Comparative study of αr -SDC, αw-SDC, r-SDC and α -GSC(N,6) receiver structures for BPSK in Vehicular A UMTS WCDMA channels mode and Rayleigh fading.

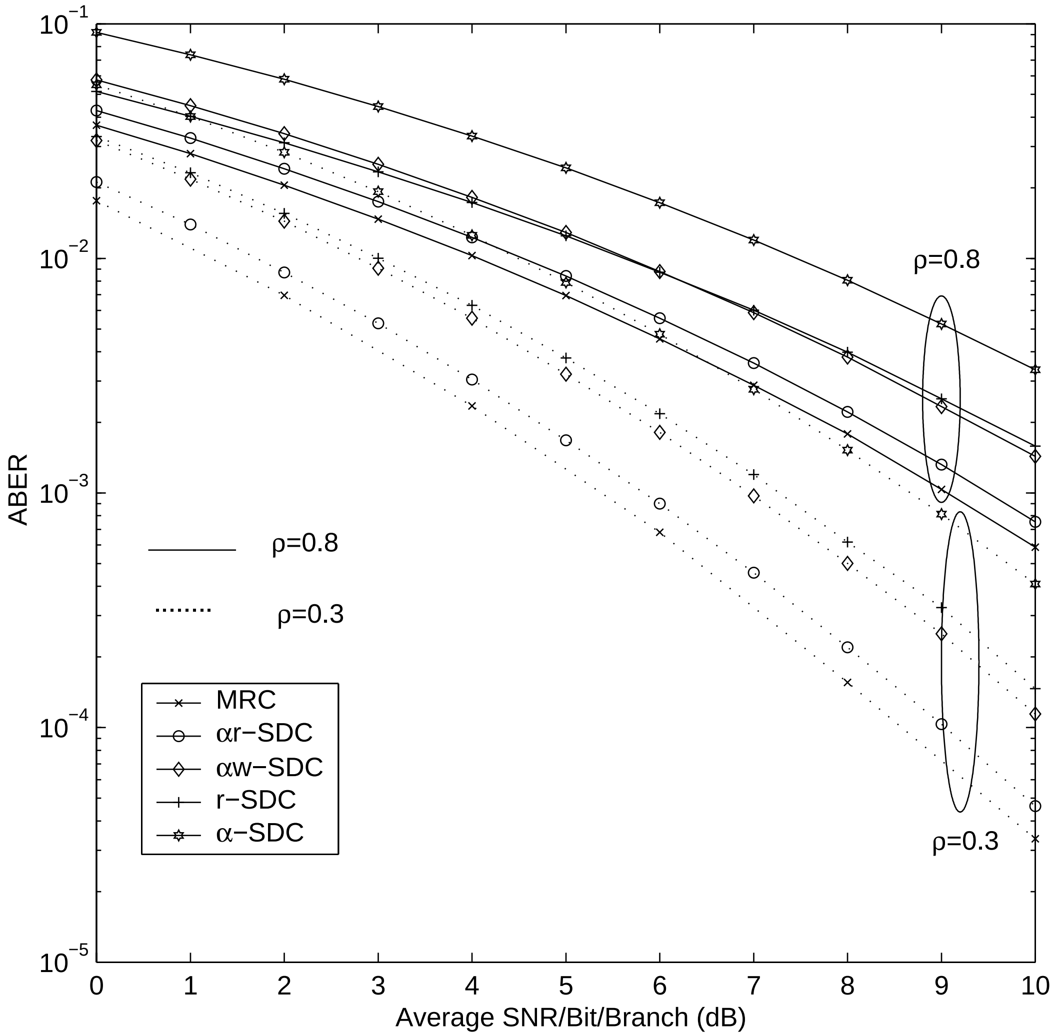

Figure 4.4 Effect of branch correlation on the ABER performance of MRC, αr -SDC, αw-SDC, α -SDC and r-SDC receiver structures when L=4 and identical mean received signal strengths (i.e., uniform MIP) across the diversity paths.

Chapter 5

DIVERSITY RECEIVER PERFORMANCE OVER NAKAGAMI-*m* FADING CHANNELS

In this chapter, analytical expressions of ABER for diversity receiver structures over Nakagami-*m* fading channels with i.n.d diversity paths are presented, the receivers under consideration include αr -SDC, α -SDC, α -GSC, *r*-SDC and MRC, the effect of branch correlations is also investigated for diversity order lager than 2. Both computational and Monte-Carlo simulation results are plotted to validate the derivation obtained in this thesis.

5.1 Performance Analysis over Nakagami-*m* Fading

- αr -SDC

In Chapter 3, the ABER of BPSK for receiver employing αr -SDC scheme is given by (3-9), $f_{\alpha_i r_i}(\cdot)$ can be evaluated in closed-form through convolution of Gaussian and Nakagami-*m* PDFs since $\alpha_i r_i = \alpha_i^2 \cdot \sqrt{E_b} + \alpha_i n_i$, viz.,

$$\begin{aligned} f_{\alpha_i r_i}(y) &= \int_0^\infty \frac{1}{\sqrt{2\pi\alpha_i^2 N_0/2}} \exp\left(-\frac{\left(y-\alpha_i^2\sqrt{E_b}\right)^2}{\alpha_i^2 N_0}\right) \frac{2m_i^{m_i}\alpha_i^{2m_i-1}}{\Gamma(m_i)\Omega_i^{m_i}} \exp\left(-\frac{m_i\alpha_i^2}{\Omega_i}\right) d\alpha_i \\ &= \frac{2m_i^{m_i}}{\sqrt{\pi N_0}\Gamma(m_i)\left(\Omega_i E_b + m_i N_0\right)^{(2m_i-1)/4}\Omega_i^{(2m_i+1)/4}} |y|^{2m_i-1} \\ &\quad \times \exp\left(2y\sqrt{E_b}/N_0\right) K_{(2m_i-1)/2}\left(\frac{2|y|}{N_0}\sqrt{\frac{\Omega_i E_b + m_i N_0}{\Omega_i}}\right) \end{aligned} \tag{5-1}$$

where $K_v(\cdot)$ denotes the modified Bessel function of the second kind of order v.The above simplification is obtained with the aid of identity [21, eq. (3.478)]:

$$\int_0^\infty x^{v-1}\exp\left(-\lambda x^p-\mu x^{-p}\right)dx=\frac{2}{p}\left(\frac{\mu}{\lambda}\right)^{\frac{v}{2p}}K_{\frac{v}{p}}\left(2\sqrt{\lambda\mu}\right)\quad \mathrm{Re}\{\lambda\}>0,\mathrm{Re}\{\mu\}>0 \qquad (5\text{-}2)$$

Moreover, note that for positive integer m_i, $K_{n+1/2}(\cdot)$ can be further expressed in terms of simple algebraic functions by utilizing identity [21, eq. (8.468)]:

$$K_{n+1/2}(z)=\sqrt{\frac{\pi}{2z}}\exp(-z)\sum_{k=0}^{n}\frac{(n+k)!}{(2z)^k\,k!(n-k)!} \qquad (5\text{-}3)$$

where n is a non-negative integer.

Substituting (5-3) into (5-1), $f_{\alpha_i r_i}(\cdot)$ can be simplified as

$$\begin{aligned}f_{\alpha_i r_i}(x)=&\frac{m_i^{m_i}}{\Gamma(m_i)\left(\Omega_i E_b+m_i N_0\right)^{m_i/2}\Omega_i^{m_i/2}}|x|^{m_i-1}\exp\left(\frac{2x\sqrt{E_b}}{N_0}-\frac{2|x|}{N_0}\sqrt{\frac{\Omega_i E_b+m_i N_0}{\Omega_i}}\right)\\&\times\exp\left(\frac{2x\sqrt{E_b}}{N_0}-\frac{2|x|}{N_0}\sqrt{\frac{\Omega_i E_b+m_i N_0}{\Omega_i}}\right)\sum_{k=0}^{m_i-1}\frac{(m_i+k-1)!}{k!(m_i-k-1)!\left(\frac{4|x|}{N_0}\sqrt{\frac{\Omega_i E_b+m_i N_0}{\Omega_i}}\right)^k}\end{aligned} \qquad (5\text{-}4)$$

For this case, $F_{|\alpha_j r_j|}(\cdot)$ can also be evaluated in closed-form using using the following relationship:

$$\int_0^u x^n e^{-\mu x}dx=\frac{n!}{\mu^{n+1}}-e^{-u\mu}\sum_{k=0}^{n}\frac{n!}{k!}\frac{u^k}{\mu^{n-k+1}} \qquad (5\text{-}5)$$

Hence, if the fading severity of the i-th diversity path assumes a positive integer value, $F_{|\alpha_i r_i|}(\cdot)$ can be evaluated in closed-form as

$$
\begin{aligned}
F_{|\alpha_j r_j|}(x) = &\left[\frac{(n_j-k)!}{\left(d_j + 2\sqrt{E_b}/N_0\right)^{n_j+1-k}} - e^{-x\left(d_j+2\sqrt{E_b}/N_0\right)} \times \sum_{l=0}^{n_j-k} \frac{(n_j-k)!\,r^l}{l!\left(d_j+2\sqrt{E_b}/N_0\right)^{n_j+1-k-l}} \right] \\
&\times \sum_{k=0}^{n_j} a_j b_j^{c_j} \sqrt{\frac{\pi}{2d_j}} \frac{(n_j+k)!}{k!(n_j-k)!(2d_j)^k} \\
&+ \left[\frac{(n_j-k)!}{\left(d_j - 2\sqrt{E_b}/N_0\right)^{n_j+1-k}} - e^{-x\left(d_j-2\sqrt{E_b}/N_0\right)} \times \sum_{l=0}^{n_j-k} \frac{(n_j-k)!\,r^l}{l!\left(d_j-2\sqrt{E_b}/N_0\right)^{n_j+1-k-l}} \right] \\
&\times \sum_{k=0}^{n_j} a_j b_j^{c_j} \sqrt{\frac{\pi}{2d_j}} \frac{(n_j+k)!}{k!(n_j-k)!(2d_j)^k}
\end{aligned}
\tag{5-6}
$$

where $m_i \in \{1,2,3\cdots\}, i=1,\cdots,L$; $a_i = \frac{2m_i^{m_i}}{\sqrt{\pi N_0}\Gamma(m_i)\Omega_i^{m_i}}$, $b_i = \frac{\Omega_i}{\Omega_i E_b + m_i N_0}$, $c_i = \frac{2m_i - 1}{4}$,

$d_i = \frac{2}{N_0}\sqrt{\frac{\Omega_i E_b + m_i N_0}{\Omega_i}}$ and $n_i = m_i - 1$.

For the special case of i.i.d Rayleigh fading, it is easy to verify that (5-4) and (5-6) reduces to [7, Eq. (20)] and [7, Eq. (21)] respectively, by setting $\Omega_i = 1$ and $m_i = 1$ for all $i = 1,2,\cdots,L$.

- α -SDC

If we assume $\sqrt{E_b}$ was transmitted (without loss of generality), and substitute the PDF and CDF of SNR with Nakagami-*m* distributed fading amplitude, the ABER of α -SDC is given by [18]

$$
P_b = \sum_{i=1}^{L} \int_0^\infty \frac{1}{2} \operatorname{erfc}\left(\sqrt{\gamma_i}\right) \frac{m_i^{m_i} \gamma_i^{m_i-1}}{\Gamma(m_i)\bar{\gamma}_i^{m_i}} \exp\left(-\frac{m_i \gamma_i}{\bar{\gamma}_i}\right) \left[\prod_{j=1, j\neq i}^{L} \frac{\gamma\left(m_j, m_j \gamma_i / \bar{\gamma}_j\right)}{\Gamma(m_j)} \right] d\gamma_i \tag{5-7}
$$

when $m_i \in \{1,2,...\}$, (5-7) can be simplified as

$$P_b = \sum_{i=1}^{L} \int_0^{\infty} \frac{1}{2} \mathrm{erfc}\left(\sqrt{\gamma_i}\right) \frac{m_i^{m_i} \gamma_i^{m_i - 1}}{\Gamma(m_i) \overline{\gamma}_i^{m_i}} \exp\left(-\frac{m_i \gamma_i}{\overline{\gamma}_i}\right)$$
$$\prod_{j=1, j\neq i}^{L} \left[1 - \exp\left(-\frac{m_j \gamma_i}{\overline{\gamma}_j}\right) \sum_{k=0}^{m_j - 1} \frac{1}{k!} \left(-\frac{m_j \gamma_i}{\overline{\gamma}_j}\right)^k \right] d\gamma_i \tag{5-8}$$

- α -GSC

If we consider α -GSC(*N,L*) scheme (*N* out of *L* paths with the largest SNRs are selected and combined in a similar fashion to MRC), it is possible to show that the ABER of BPSK with α -GSC(*N,L*) receiver over general independent fading channels is given by (3-13), viz.,

$$P_b = \frac{1}{\pi} \int_0^{\pi/2} \phi_\gamma \left(\frac{1}{\sin^2 \theta} \right) d\theta \tag{5-9}$$

where $\phi_\gamma(\cdot)$ denotes the moment generating function of (MGF) α -GSC(*N,L*) output SNR

$$\phi_\gamma(s) = \sum_{\tau \in T_{L,N}} \int_0^{\infty} e^{-sx} f_{\tau(L-N+1)}(x) \left[\prod_{i=1}^{L-N} F_{\tau(i)}(x) \right] \prod_{k=L-N+2}^{L} \phi_{\tau(k)}(s,x) dx \tag{5-10}$$

where the PDF $f_i(\cdot)$, the CDF $F_i(\cdot)$ and marginal MGF $\phi_i(s,x)$ of γ_i are given by

$$f_i(x) = \frac{m_i^{m_i} x^{m_i - 1}}{\Gamma(m_i) \overline{\gamma}_i^{m_i}} \exp\left(-\frac{m_i x}{\overline{\gamma}_i}\right)$$
$$F_i(x) = \frac{\gamma\left(m_i, m_i x / \overline{\gamma}_i\right)}{\Gamma(m_i)} \tag{5-11}$$
$$\phi_i(s,x) = \frac{1}{\Gamma(m_i)} \left(\frac{m_i}{m_i + s\overline{\gamma}_i} \right)^{m_i} \Gamma\left(m_i, sx + x\, m_i / \overline{\gamma}_i\right)$$

where $\Gamma(a,x) = \int_x^{\infty} \exp(-t) t^{a-1} dt$ denotes the complementary incomplete Gamma function.

- r-SDC

The generic formula for r-SDC over Nakagami-m fading channels is given in (3-15), we need to find the PDF of random variable of $z_i = r_i \big/ \sqrt{N_0/2}$, it can be written as

$$\begin{aligned} g(z_i) &= \int_0^{\infty} \frac{1}{\sqrt{2\pi}} \exp\left(-\frac{(z_i - y)^2}{2}\right) \frac{2m_i^{m_i}}{\Gamma(m_i)(2\overline{\gamma}_i)^{m_i}} y^{2m_i-1} \exp\left(-\frac{m_i y^2}{2\overline{\gamma}_i}\right) dy \\ &= \frac{2\Gamma(2m_i)}{\sqrt{2\pi}\Gamma(m_i)} \left(\frac{m_i}{2(m_i+\overline{\gamma}_i)}\right)^{m_i} \exp\left(-\frac{z_i^2(2m_i+\overline{\gamma}_i)}{4(m_i+\overline{\gamma}_i)}\right) D_{-2m_i}\left(-z_i\sqrt{\frac{\overline{\gamma}_i}{m_i+\overline{\gamma}_i}}\right) \end{aligned} \tag{5-12}$$

The parabolic cylinder function $D_v(\cdot)$ in (5-12) can be evaluated using

$$\begin{aligned} D_v(z) &= \frac{\Gamma(0.5)2^{v/2+1/4}z^{-1/2}}{\Gamma(0.5-0.5v)} {}_1F_1\left(\frac{1}{2}v+\frac{1}{4};-\frac{1}{4};\frac{1}{2}z^2\right) \\ &\quad + \frac{\Gamma(-0.5)2^{v/2+1/4}z^{-1/2}}{\Gamma(-0.5v)} {}_1F_1\left(\frac{1}{2}v+\frac{1}{4};\frac{1}{4};\frac{1}{2}z^2\right) \end{aligned} \tag{5-13}$$

where ${}_1F_1(.;.;.)$ is the confluent hypergeometric function defined as

$${}_1F_1 = (a;b;z) = \frac{\Gamma(b)}{\Gamma(b-a)\Gamma(a)} \int_0^1 e^{zt} t^{a-1} (1-t)^{b-a-1} dt \tag{5-14}$$

- MRC

If we substitute the MGF of instantaneous SNR of the i-th path into (3-19), the ABER for MRC diversity receiver is obtained as

$$P_b = \frac{1}{\pi} \int_0^{\pi/2} \prod_{i=1}^{L} \left(\frac{m_i \sin^2\theta}{m_i \sin^2\theta + \overline{\gamma}_i}\right)^{m_i} d\theta \tag{5-15}$$

5.2 Effect of Branch Correlations on Receiver Diversity Performance

Like the case in Rayleigh fading channels, it is difficult to find the analytical expressions for diversity receivers with diversity order larger than 2, hence we present analytical expressions for computing the ABER of a dual diversity BPSK in conjunction with αr-SDC, α-SDC and *r*-SDC over correlated Nakagami-*m* fading channels.

Since the maximum of $|\alpha_1 r_1|$ and $|\alpha_2 r_2|$ dominates the sign of $\alpha_1 r_1 + \alpha_2 r_2$, the ABER of BPSK that employs dual-diversity αr-SDC is essentially the ABER of BPSK with dual-diversity MRC, it can be evaluated using (4-13), for the case of correlated Nakagami-*m* fading environment with identical fading index *m*, the marginal MGF $\phi_\gamma(\cdot)$ in (4-13) is given by[24]

$$\phi_\gamma(s) = \frac{m^m}{\left[\bar{\gamma}_1\bar{\gamma}_2(1-\rho)\left(\left(s+\frac{\bar{\gamma}_1+\bar{\gamma}_2}{2\bar{\gamma}_1\bar{\gamma}_2\rho}\right)^2 - \frac{(\bar{\gamma}_1-\bar{\gamma}_2)^2+4\bar{\gamma}_1\bar{\gamma}_2\rho}{4\bar{\gamma}_1^2\bar{\gamma}_2^2(1-\rho)^2}\right)\right]^m} \tag{5-16}$$

For α-SDC, the ABER of BPSK is readily computed using (4-13) except that $\phi_\gamma(\cdot)$ is given by [23, eq. (30)]

$$\phi_\gamma(s) = \frac{2^{2m}\Gamma(2m)}{\Gamma(m)\Gamma(m+1)}\,{}_2F_1\left(1-m, m; 1+m; \frac{1-1/B_{ij}}{2}\right)\sum_{i=1, j\neq i}^{2}\frac{A_{ij}^{2m}}{\left[\bar{\gamma}_i B_{ij}\left(1+B_{ij}\right)\right]^m} \tag{5-17}$$

where ${}_2F_1(.;.;.)$ is the Gaussian hypergeometric function, $A_{ij} = \dfrac{\sqrt{\bar{\gamma}_j(1-\rho)/2}}{\bar{\gamma}_j/\bar{\gamma}_i - 1 + s\bar{\gamma}_j(1-\rho)}$ and

$$B_{ij} = \frac{\sqrt{\left[s\bar{\gamma}_i\bar{\gamma}_j(1-\rho)+\bar{\gamma}_i+\bar{\gamma}_j\right]^2 - 4\rho\bar{\gamma}_i\bar{\gamma}_j}}{s\bar{\gamma}_i\bar{\gamma}_j(1-\rho)+\bar{\gamma}_j-\bar{\gamma}_i}.$$

Similarly, the ABER performance of dual-diversity *r*-SDC for BPSK over Nakagami-*m* fading channels can be computed as [27, eq(12)]

$$P_b = \frac{1}{2} - \frac{\sqrt{2}}{2}\sum_{k=1}^{\infty}\frac{4^{2-k-m}\rho^{k-1}(1-\rho)^{1.5-k}\,\Gamma(2k+2m-2)}{\Gamma(m)\Gamma(k)\Gamma(m+k-0.5)\Gamma^2(m+k-1)} \times \sum_{i=1, j\neq i}^{2}\sqrt{\frac{\overline{\gamma}_j\pi}{B}}F_2\left(\frac{1}{2};\frac{3}{2}-k-m, 2-k-m;\frac{1}{2},\frac{3}{2};\frac{A\overline{\gamma}_i}{B},\frac{A\overline{\gamma}_j}{B}\right) \quad (5\text{-}18)$$

where $A=(1-\rho)/2$, $B=1+A(\overline{\gamma}_1+\overline{\gamma}_2)$ and $F_2(.;.;.;.)$ denotes the Appell's hypergeometric function.

For higher diversity orders, the analysis of αr -SDC and *r*-SDC with correlated diversity paths do not appear to be tractable using an analytical approach. As such, we resort to the simulation technique to study the effect of branch correlations on the receiver performance.

5.3 Analytical and Simulation Results

- The Diversity Order

Figure 5.1 illustrates the ABER performance curves for diversity BPSK over Nakagami-*m* fading (*m* = 2) with i.i.d fading statistics. Although MRC and αr -SDC yield identical performance for *L* = 2, their discrepancy gets larger as the order of diversity increases. For example, 4th order αr -SDC, αw-SDC, *r*-SDC and α -SDC receivers incur mean SNR/bit/branch penalties of 0.5 dB, 2.1 dB, 1.8 dB and 4.2 dB respectively, with respect to MRC at ABER of 10^{-6}. While αw-SDC outperforms *r*-SDC in Rayleigh fading with i.i.d fading statistics and their difference becomes more pronounced with increasing order of diversity, we found that *r*-SDC performs slightly better than αw-SDC as the channel condition improves (i.e., a larger *m* value) and for small/moderate diversity orders. Also, the difference between α -SDC and ABER curves of other selection methods (*r*-SDC, αr -SDC and αw-SDC) widens with increasing *L*. This may be attributed to the increased number of choices among statistically independent Gaussian noise samples in the latter selection schemes.

- Power Decay Factor

Figure 5.2 examines the impact of dissimilar mean received signal strengths on diversity BPSK performance over a Nakagami-*m* fading channel (*m* = 2) and *L* = 4. As expected, there is some loss in diversity gain due to power imbalance across the diversity paths. It is also apparent from this figure that αr-SDC yields comparable performance to the optimal linear diversity combiner as the channel becomes less dispersive despite *L* = 4. This observation can be attributed to the following two trends: (a) the relative diversity improvement declines with increasing *L*; (b) the statistical diversity advantage is maximum when $\delta = 0$ and relative improvement decreases with increasing δ. Different from the i.i.d diversity paths case, *r*-SDC does not always perform better than α-SDC particularly for large δ and small average SNR/bit values. This trend is in agreement with the observation cited in [18]. From Figure 5.2, we can also conclude that both αr-SDC and αw-SDC are much more robust against variations in the mean received signal strengths across the diversity paths compared to the *r*-SDC method.

- Influence of the Fading Severity Index

The effects of fading severity index *m* on ASER of various receiver structures are illustrated in Figure 5.3. Although the receiver performance is always better in a Nakagami-m channel with a higher fading index, the relative diversity improvement, however, is greater in a channel that experience more severe fading (not shown in the figure). When *m* = 2, MRC outperforms αr-SDC, *r*-SDC, αw-SDC and α-SDC schemes by 0.6 dB, 1.7 dB, 2.1 dB and 4.0 dB respectively at ABER of 10^{-5}. When *m* = 4, the corresponding average SNR/bit penalties are 0.7 dB, 1.5 dB, 2.4 dB and 4.3 dB respectively at the same ABER. Since the spread between αw-SDC (or α-SDC) and αr-SDC (or *r*-SDC) becomes wider as *m* increases, we may conclude that SDC schemes that do not require phase compensation during the selection process are more susceptible to the variations in the fading severity index. It is also interesting to note that for a fixed *L*, the difference between *r*-SDC and MRC performance curves decreases as *m* increases. This is in contrast to the trend exhibited by other selection schemes.

- Performance Compared to GSC receiver

Figure 5.4 provides diversity BPSK performance curves for several receiver structures in a Nakagami-m channel (*m* = 2) to facilitate a comparative study of all the diversity methods in terms of ABER metric. Contrary to [19], we observe that *r*-SDC starts to perform better than αw-SDC when the channel experiences fewer deep fades. Both *r*-SDC and αw-SDC yield performance comparable to α-GSC(2,7) but with simpler receiver designs. It is also apparent that ABER of αr-SDC is bounded by α-GSC(3,7) and α-GSC(4,7) performance curves. Moreover, αr-SDC is only 1.6 dB and 0.4 dB (i.e., SNR penalty) inferior to MRC and α-GSC(4,7) respectively, at ABER of 10^{-5}. Therefore αr-SDC, αw-SDC and *r*-SDC schemes represent viable alternatives for receiver designs that currently employ α-GSC(*N*,*L*) since they achieve good performance with considerably less hardware and computational delay.

- Impact of Branch Correlation

Figure 5.5 depicts the diversity BPSK performance in a correlated Nakagami-*m* fading channel (*m* = 2). To generate this plot, we have assumed *L* = 4, uniform MIP and constant correlation model with power correlation coefficient ρ. When $\rho = 0.3$, MRC outperforms αr-SDC, *r*-SDC, αw-SDC and α-SDC by 0.6 dB, 1.4 dB, 1.9 dB and 4 dB respectively, at ABER of 10^{-3}. When ρ=0.8, the corresponding average SNR/bit/branch penalties (at the same ABER) are 0.7 dB, 1.3 dB, 2.1 dB and 4.2 dB respectively. Thus, we may deduce that αw-SDC and α-SDC are more vulnerable to branch correlations compared to αr-SDC and *r*-SDC schemes (i.e., since the spread between αw-SDC or α-SDC and MRC performance curves increases for higher ρ). Moreover, we found that *r*-SDC to be most robust against branch correlations compared to all other SDC methods.

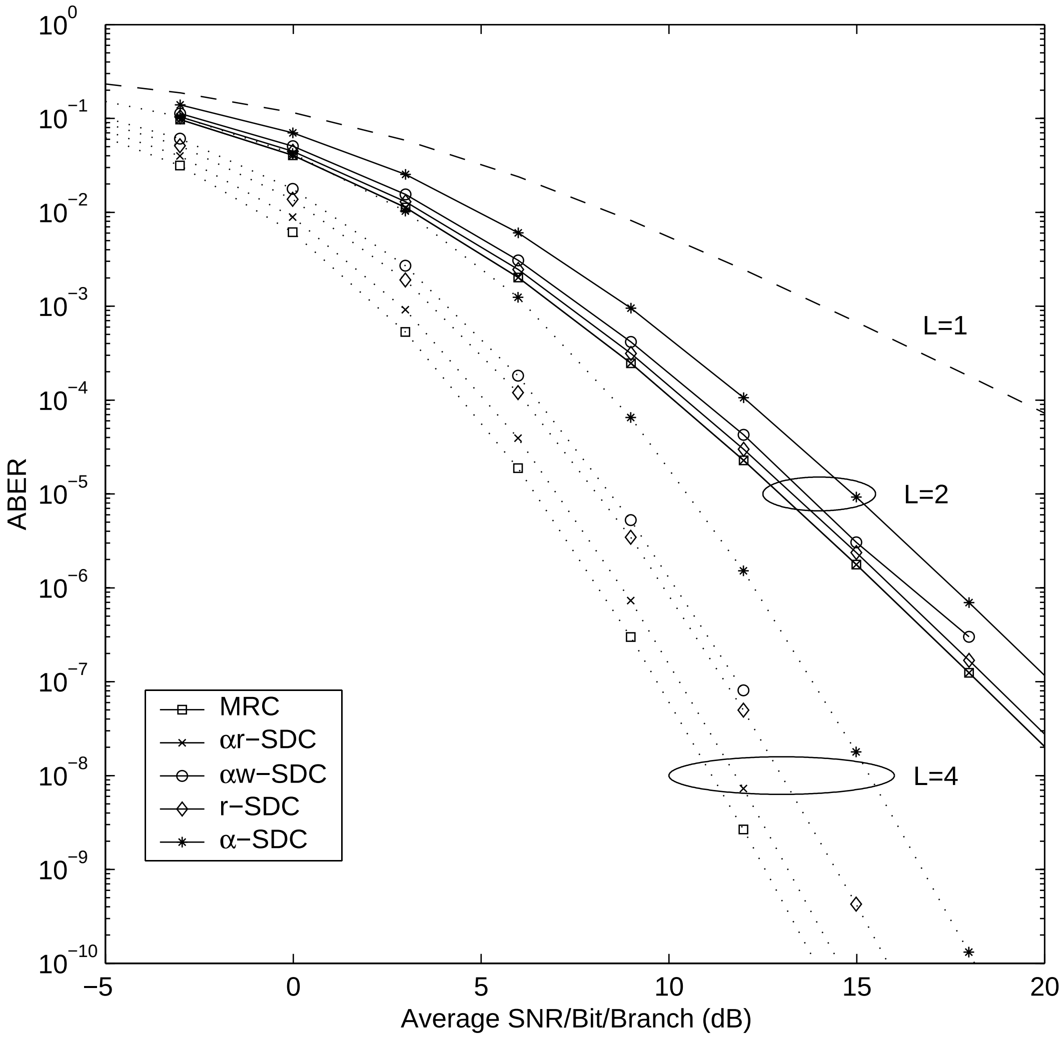

Figure 5.1 ABER plotted of BPSK over i.i.d Nakagami-*m* channels (m=2) for different receiver structures and diversity order L.

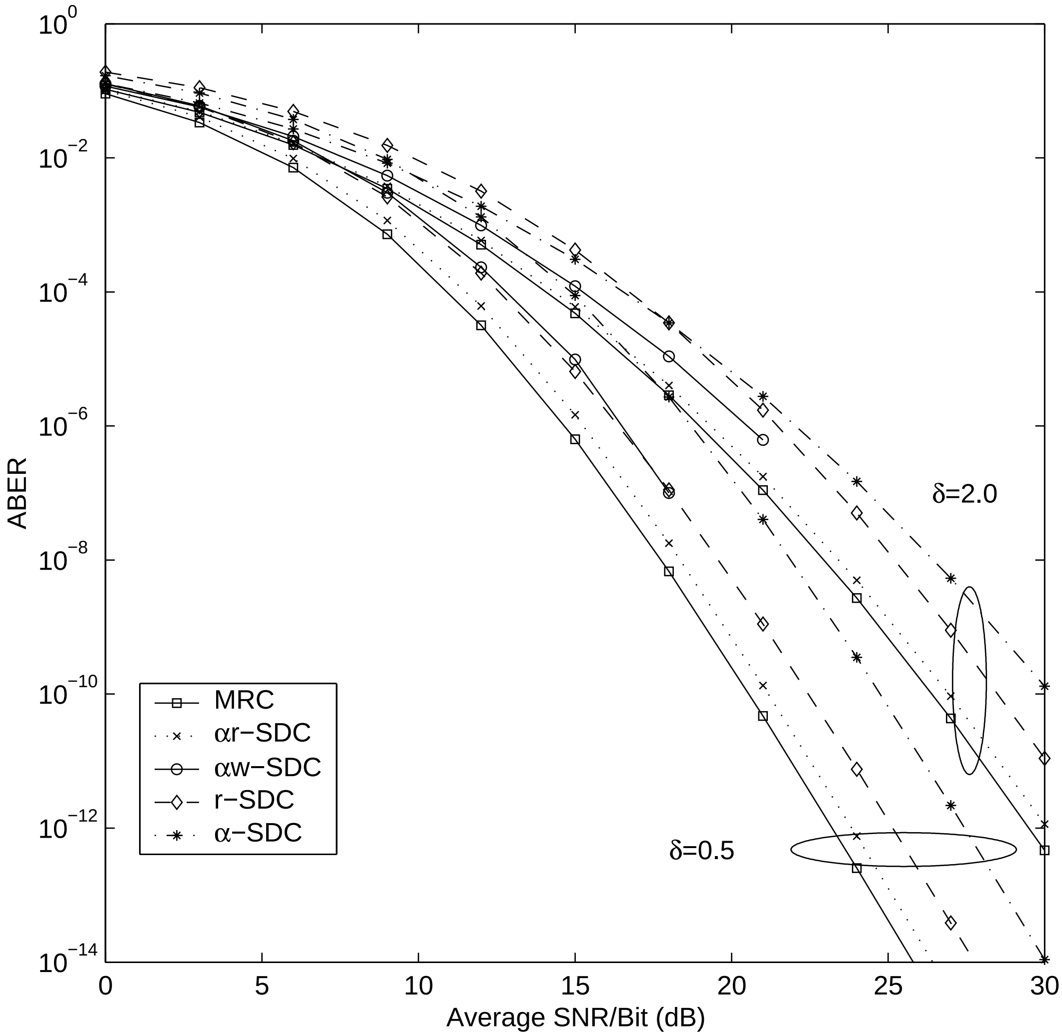

Figure 5.2 ABER of BPSK over Nakagami-*m* channels (*m*=2) with *L*=4 i.n.d diversity paths for two different δ values.

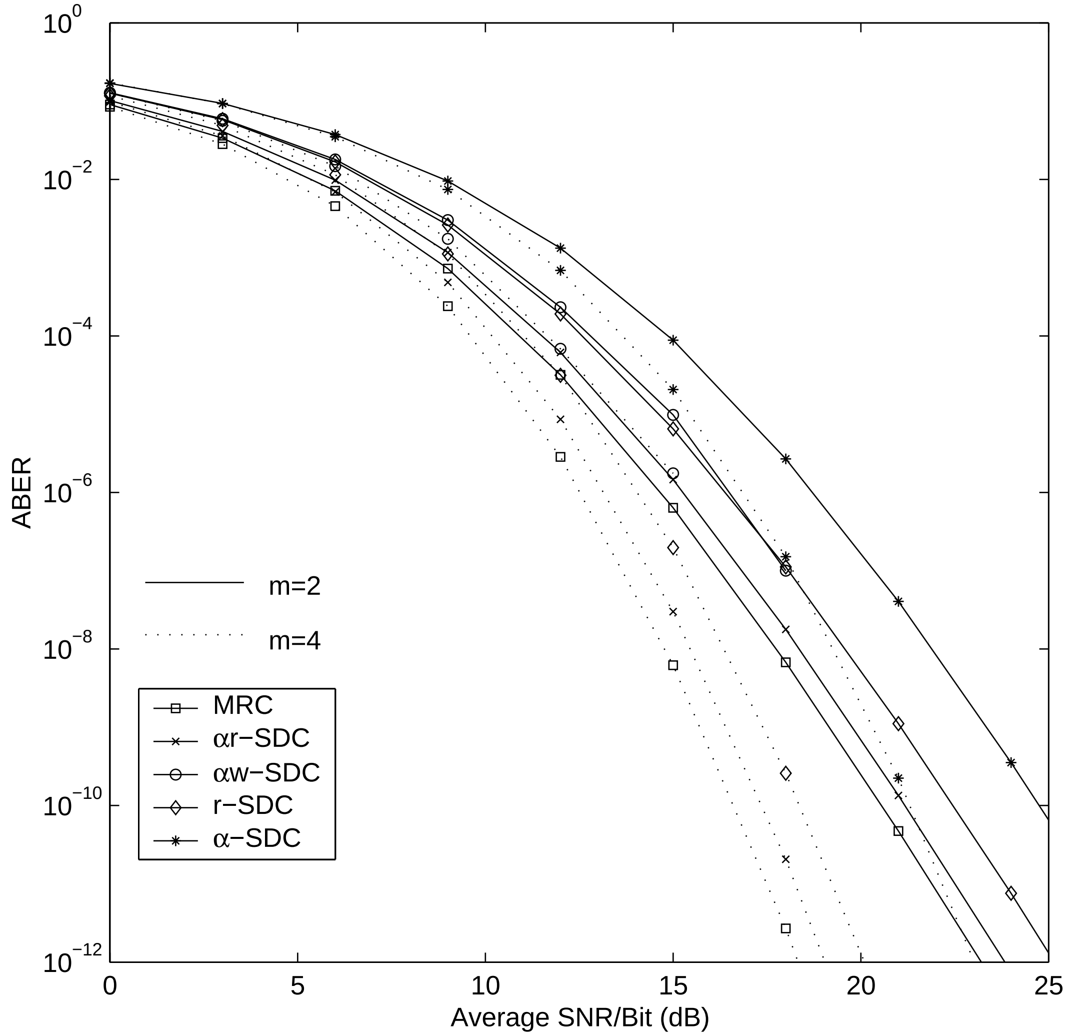

Figure 5.3 ABER performance curves for BPSK over Nakagami-*m* channels with *L*=4 and $\delta = 0.5$.

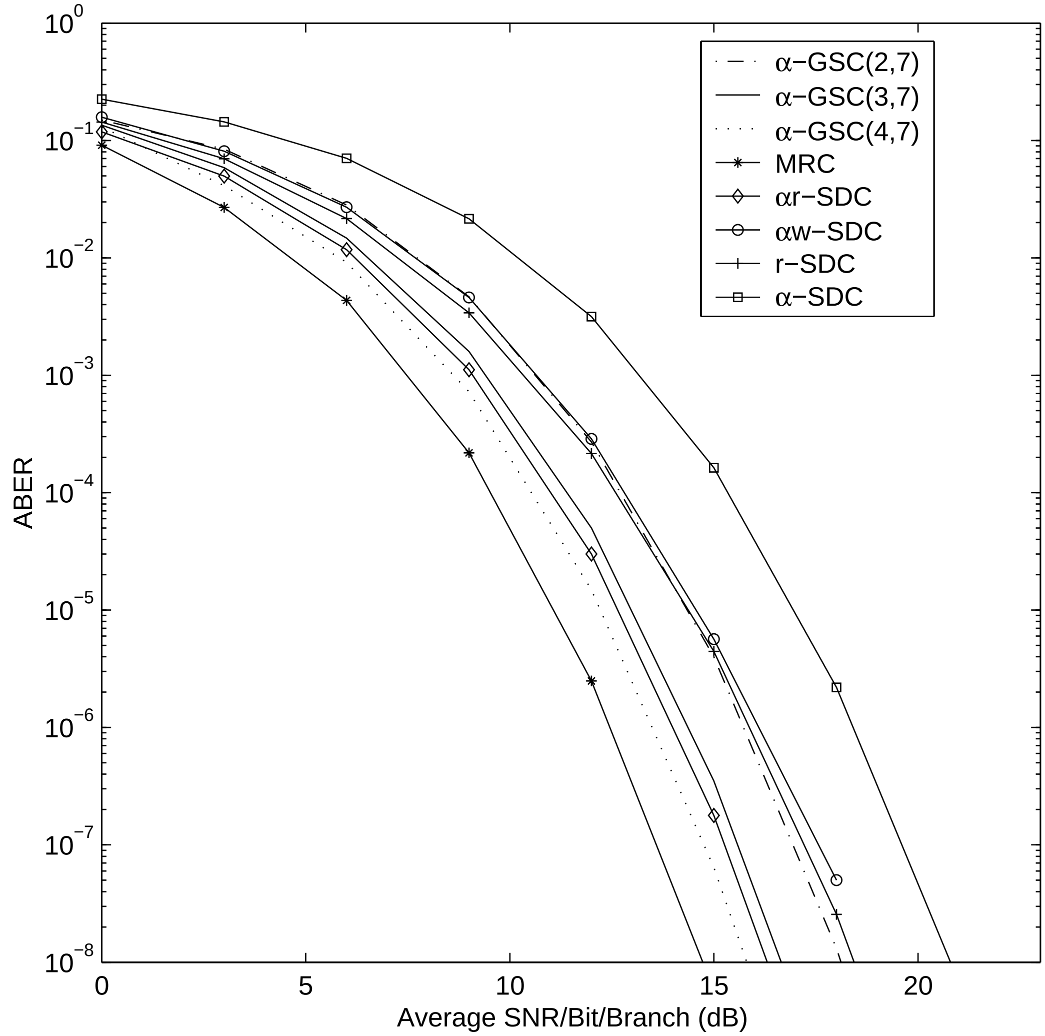

Figure 5.4 Comparative study of αr-SDC, αw-SDC, r-SDC and α-GSC(N,7) receiver structures for BPSK modulation scheme over Nakagami-m channels (m=2) and uniform MIP($\delta = 0$).

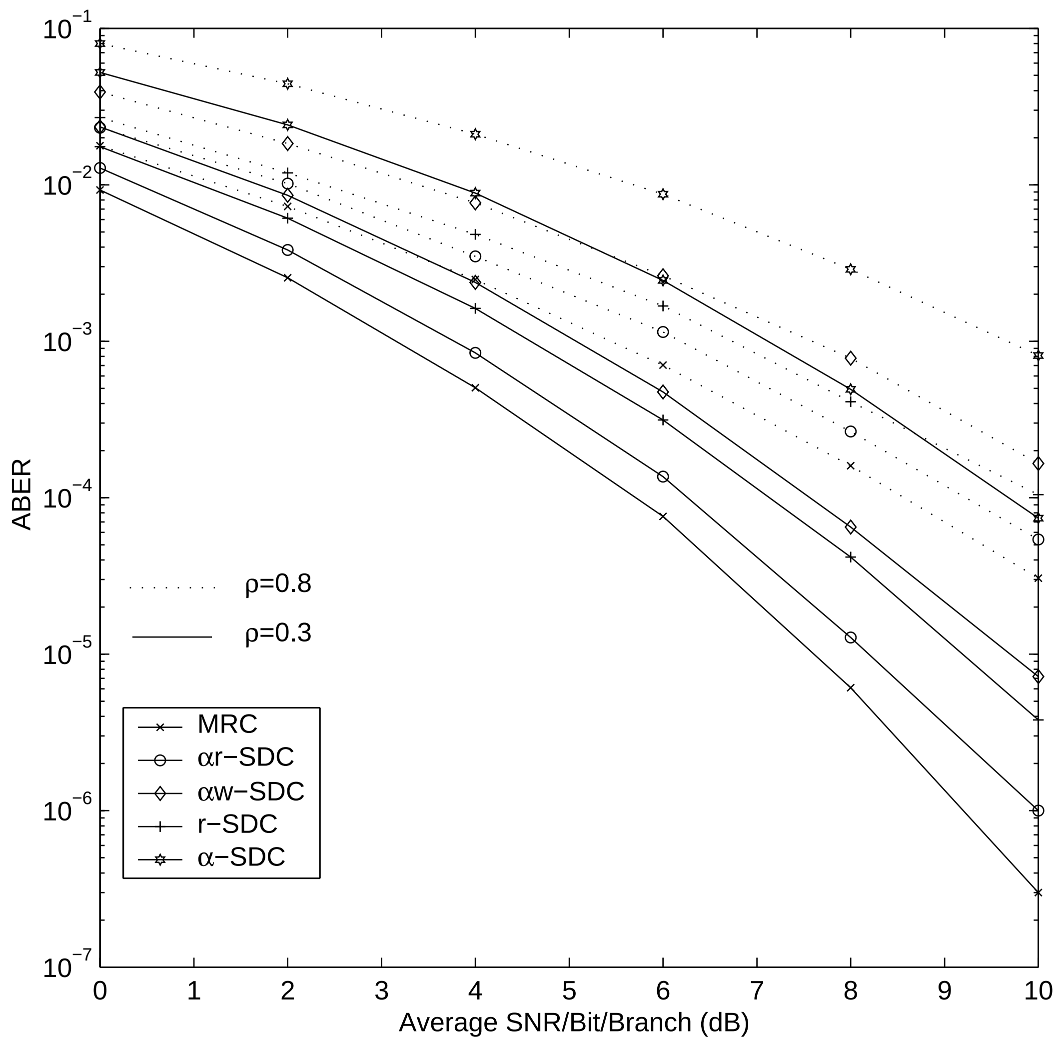

Figure 5.5 Effect of branch correlation on the ABER performance of different selection combining schemes when L=4 with identical mean received signal strengths across diversity paths and Nakagami-m fading severity index m=2.

Chapter 6

DIVERSITY RECEIVER PERFORMANCE OVER RICEAN FADING CHANNELS

6.1 Performance Analysis over Ricean Fading Channels

- αr -SDC

Following the derivations in Chapter 3, the ABER expression for receiver employing αr -SDC in Ricean fading channels with i.n.d diversity paths is given in (3-9), where the PDF of $\alpha_i r_i$, $f_{\alpha_i}(\alpha_i)$, is given by

$$
\begin{aligned}
f_{\alpha_i r_i}(y) &= \int_0^\infty \frac{1}{\sqrt{\pi N_0}} \cdot \exp\left(-\frac{\left(y - \alpha_i^2 \sqrt{E_b}\right)^2}{\alpha_i^2 N_0} \right) \\
&\quad \times \frac{2(1+K_i)}{\Omega_i} \exp(-K_i) \exp\left(-\frac{(1+K_i)\alpha_i^2}{\Omega_i} \right) I_0\left(2\alpha_i \sqrt{\frac{K_i(1+K_i)}{\Omega_i}} \right) d\alpha_i \\
&= \sum_{k=0}^{\infty} \frac{1}{\sqrt{\pi N_0}} \left(\frac{K_i(1+K_i)}{\Omega_i k! \Gamma(k+1)} \right)^k \left(\frac{y^2 \Omega_i}{E_b \Omega_i + (1+K_i) N_0} \right)^{(2k+1)/4} K_{\frac{2k+1}{2}}\left(2\sqrt{\frac{y^2}{N_0}\left(\frac{E_b}{N_0} + \frac{1+K_i}{\Omega_i} \right)} \right)
\end{aligned}
\tag{6-1}
$$

- α -SDC

Substituting the PDF and CDF of instantaneous SNR of the *i*-th path given in (2-11) and (2-12) into (3-11), we have the ABER for α -SDC over Ricean fading channels with i.n.d diversity paths

$$
\begin{aligned}
P_b &= \sum_{i=1}^{L} \int_0^\infty \frac{1}{2} \operatorname{erfc}\left(\sqrt{\gamma_i}\right) \frac{1+K_i}{\overline{\gamma}_i} \exp\left(-K_i - \frac{1+K_i}{\overline{\gamma}_i} \gamma_i \right) I_0\left(2\sqrt{\frac{K_i(K_i+1)\gamma_i}{\overline{\gamma}_i}} \right) \\
&\quad \times \prod_{j=1, j\neq i}^{L} \left[1 - Q\left(\sqrt{2K_j}, \sqrt{\frac{2(K_j+1)\gamma_i}{\overline{\gamma}_j}} \right) \right] d\gamma_i
\end{aligned}
\tag{6-2}
$$

- α -GSC

The ABER for α -GSC is given in (3-13), where the PDF and CDF of the instantaneous SNR of the *i*-th path in Ricean fading channels is given in (2-11) and (2-12) respectively, the marginal MGF is given by

$$\phi_{\gamma_i}(s,\gamma_i) = \frac{1+K_i}{s\overline{\gamma}_i + K_i + 1}\exp\left(-\frac{sK_i\overline{\gamma}_i}{s\overline{\gamma}_i + K_i + 1}\right) Q\left(\sqrt{\frac{2K_i(K_i+1)}{s\overline{\gamma}_i + K_i + 1}}, \sqrt{\frac{2(s\overline{\gamma}_i + K_i + 1)\gamma_i}{\overline{\gamma}_i}}\right) \quad (6\text{-}3)$$

- *r*-SDC

The ABER of BPSK for receiver employing *r*-SDC over Ricean fading with i.n.d diversity paths is given by (3-15), since $z_i = r_i/\sigma = \left(\alpha_i\sqrt{E_b} + n_i\right)\Big/\sqrt{N_0/2}$, we have the PDF of z_i

$$g(z_i) = \int_0^{\infty} \frac{1}{\sqrt{2\pi}} \exp\left(-\frac{(z_i - y)^2}{2}\right) f_i(y)\, dy \quad (6\text{-}4)$$

the PDF of random variable $\sqrt{\frac{2E_b}{N_0}}\alpha_i$, $f_i(\cdot)$, is of the form

$$f_i(y) = \frac{(1+K_i)y}{\overline{\gamma}_i}\exp(-K_i)\exp\left(-\frac{(1+K_i)y^2}{2\overline{\gamma}_i}\right) I_0\left(y\sqrt{\frac{2K_i(1+K_i)}{\overline{\gamma}_i}}\right) \quad (6\text{-}5)$$

- MRC

Substituting the MGF for Ricean fading given in (2-16) into expression (3-19), we have the ABER of MRC in Ricean fading channels with i.n.d diversity paths

$$P_b = \frac{1}{\pi}\int_0^{\pi/2} \prod_{i=1}^{L} \frac{(1+K_i)\sin^2\theta}{(1+K_i)+\overline{\gamma}_i} \exp\left(-\frac{K_i\overline{\gamma}_i}{(1+K_i)\sin^2\theta + \overline{\gamma}_i}\right) d\theta \quad (6\text{-}6)$$

6.2 Analytical and Simulation Results

In Figure 6.1, we study the impact of diversity order L on the ABER performance for BPSK over Ricean fading channels. We assume Ricean factor K=3 and MIP power decaying factor $\delta = 1$. For dual-diversity case, we observe that the αr-SDC yields performance identical to that of MRC, the same trend we get for Rayleigh and Nakagami-*m* fading cases. As diversity order increases to 4, αr-SDC scheme outperforms αw-SDC, *r*-SDC and α-SDC. Note that αw-SDC yields better performance than *r*-SDC and α-SDC. At ABER of 10^{-3} and L=4, αr-SDC, αw-SDC, *r*-SDC and α-SDC incur 0.5 dB, 1.3 dB, 2.1 dB and 3.0 dB penalty in terms of SNR/bit/branch with respect to MRC.

Figure 6.2 compares the ABER performance of different diversity receivers over Ricean fading environments with various power decaying factor. This plot is generated by setting the diversity order to 4, Ricean factor K=3 for all receivers considered. Since the small value of δ means the less degree of power imbalance across diversity paths, therefore , we expect better perform when $\delta = 1$ compared to $\delta = 3$. Note that for the power imbalance case, the ABER performance of αr-SDC is close to that of MRC and outperforms the rest selection schemes. It is interesting to point that when power imbalance appears manifest ($\delta = 3$), α-SDC has better performance than that of *r*-SDC for lower average SNR/bit.

The effect of Ricean factor on ABER performance for BPSK with i.n.d diversity paths over Ricean fading environments is depicted in Figure 6.3. To generate this plot, diversity order is 4, MIP parameter $\delta = 1$, as Ricean factor K increases (form 3 to 8), it is observed that all of receivers considered have better performance compared to their counterparts, this is due to the fact when K increases, it is unlikely there is larger fading amplitude, hence, the better performance is anticipated. Again, αr-SDC outperforms αw-SDC, *r*-SDC and α-SDC , αw-SDC performs better than *r*-SDC and α-SDC.

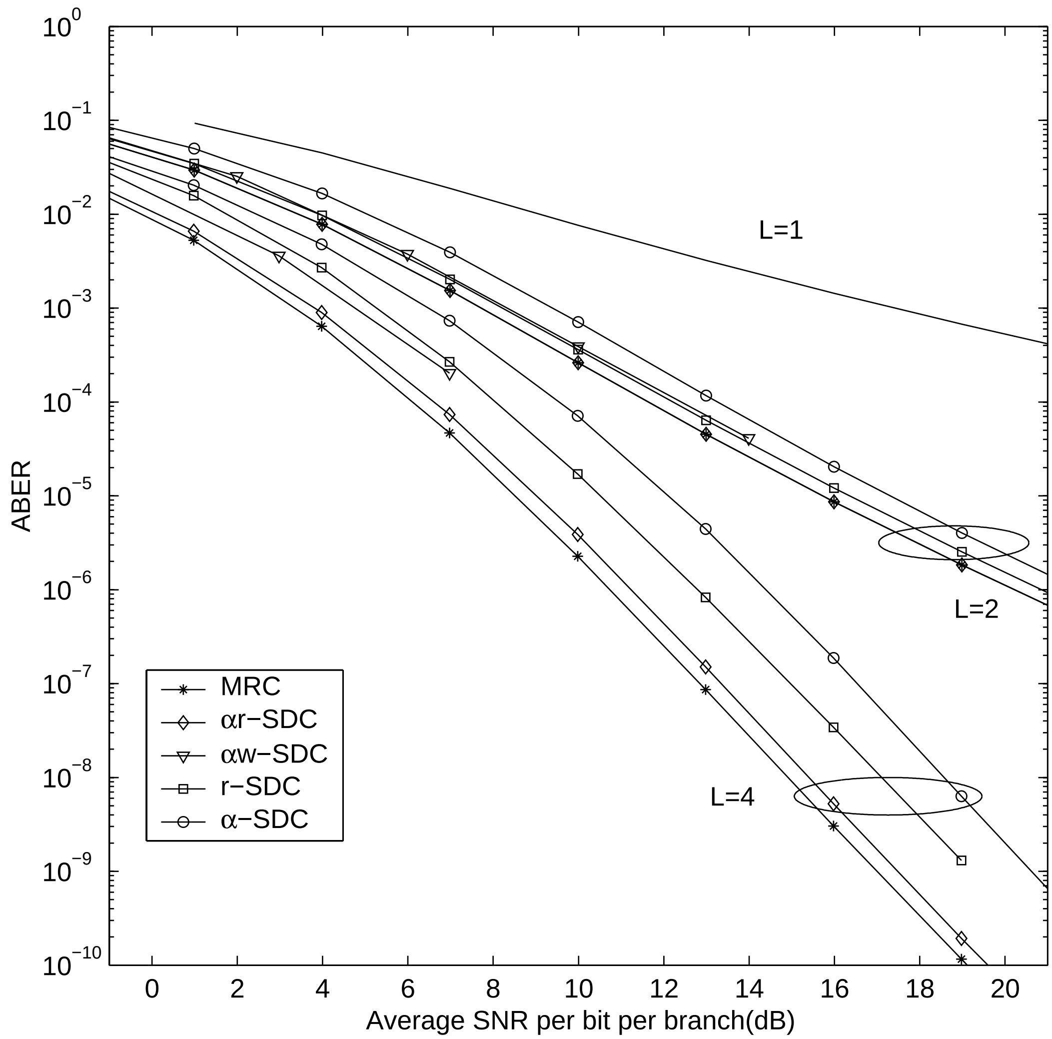

Figure 6.1 ABER performance of BPSK with i.n.d diversity paths over Ricean fading channels (K=3, $\delta = 1$).

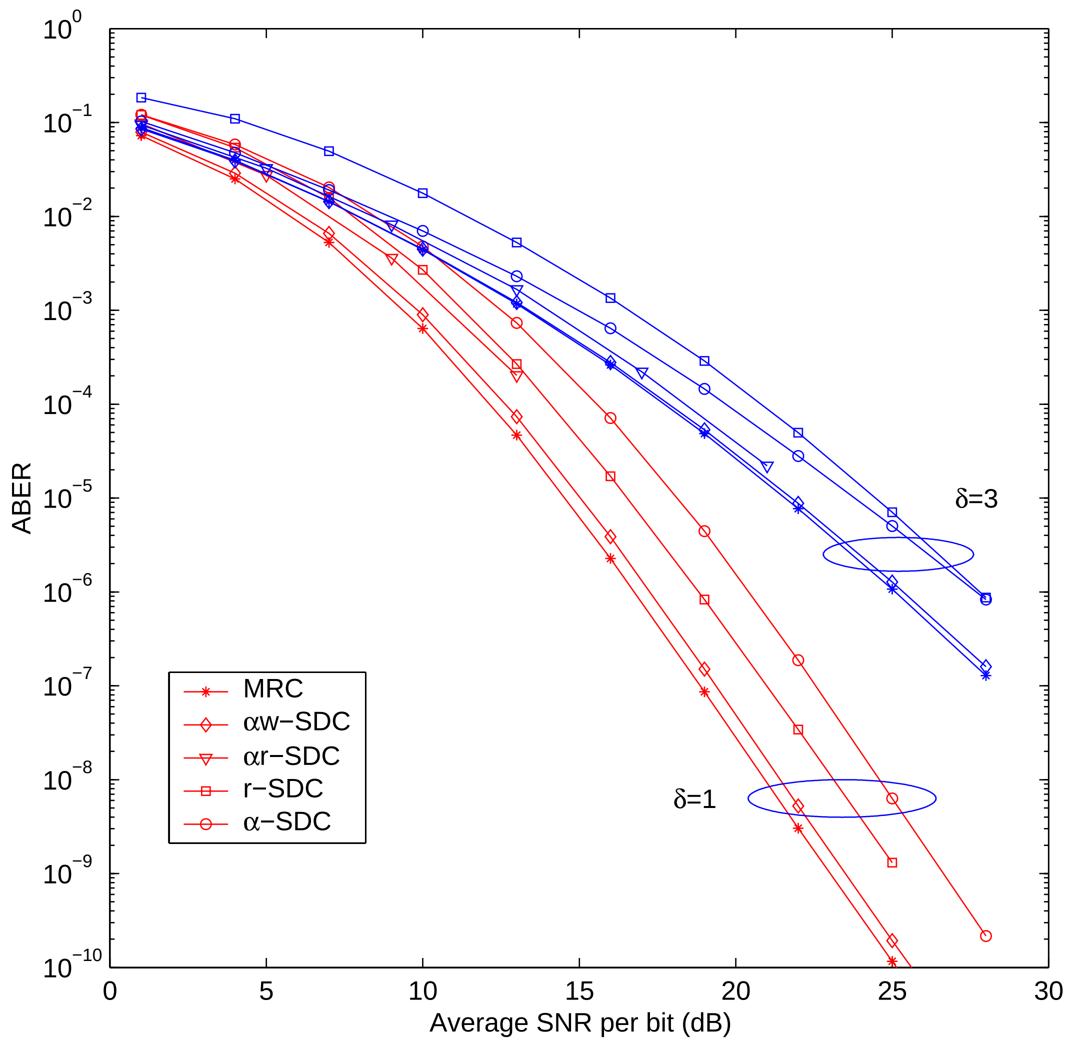

Figure 6.2 Effect of power imbalance on the performance of different receivers (L=4, K=3).

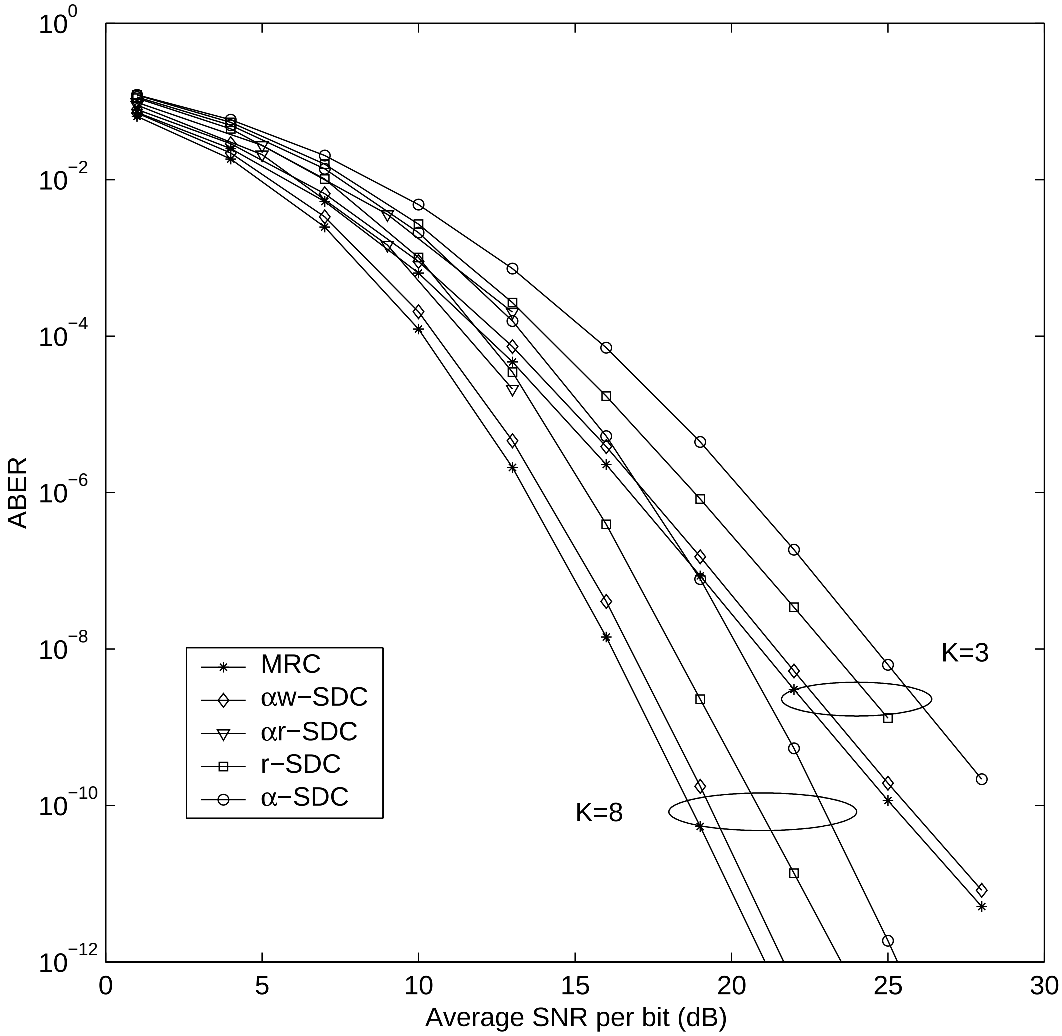

Figure 6.3 Effect of Ricean Factor on the Performance of MRC, αr -SDC, αw-SDC, r-SDC and α -SDC (L=4, $\delta = 1$).

Chapter 7

CONCLUSIONS AND FUTURE WORK

In this thesis, we extended the analysis of the new diversity selection rule based on LLR proposed by Kim. The efficacies of αr-SDC and αw-SDC schemes in Rayleigh, Nakagami-*m* and Ricean fading channels (for both independent and correlated diversity paths assumptions) are examined by comparing their performance with α-GSC(*N,L*) and *r*-SDC schemes. An attractive feature of the αr-SDC and the αw-SDC selection rules is that they yield performance comparable to the α-GSC (*N, L*) (and even with the MRC for small diversity order *L*) in practical operating environments but with considerably less hardware complexity (since they do not combine multipath signals from more than one rake finger). It is also expected that a generalized selection combining receiver based on αr and αw criterions (i.e., αr- GSC(*N,L*) or αw- GSC(*N,L*)) will yield further improvements and thereby realize performance comparable to the optimum linear diversity combiner by combining signals from only a few (finite) rake fingers. It is also observed that the αw-SDC performance is less susceptible to the variations in the mean signal strengths compared to the r-SDC selection rule. However, the αw-SDC performance is more vulnerable to branch correlations compared to the *r*-SDC scheme. For dual diversity case, αr-SDC and *r*-SDC yield performance identical to the MRC and the EGC respectively, regardless of whether the diversity paths are independent or correlated. This is particularly interesting in that the dual diversity systems are by far more common in current spatial (antenna) diversity applications.

The following lists some of possible future work for αr-SDC and αw-SDC diversity selection scheme.

- In this thesis, we examined the ABER performance of αr-SDC and αw-SDC receiver for coherent detection. Specifically, we compared the performance of αr-SDC and αw-SDC with that of MRC, *r*-SDC, α-SDC and α-GSC for coherent

BPSK. It may be informative to extend the analysis to noncoherent detection schemes such as noncoherent FSK or binary differential PSK.

- In Chapter 4, we concluded that selection rules based on LLR may reduce the number of rake fingers to achieve a prescribed ABER performance. Since αr -GSC(N,L) may yield the better performance than α -GSC(N,L), it would be interesting to extend the present analysis to GSC schemes.

- The performance of αr -SDC and αw-SDC in correlated Ricean channel is still an open issue. To this end, we have resorted to Monte-Carlo simulation method. While the literature on efficient simulation of correlated Nakagami-*m* and Rayleigh channels is quite elaborate, efficient technique for generating correlated Ricean random variables is very scare.

- The ABER performance analysis is based on perfect knowledge of channel state information, perfect symbol timing assumptions, etc. We want to study the performance of these receiver structures under non-ideal operating conditions. It is still unclear how the timing error and phase jittering will impact αr -SDC and αw-SDC receiver performance.

- To demonstrate the advantage brought by αr -SDC and αw-SDC schemes, it is advantageous to implement the new selection rules based on LLR in FPGA/DSP. This effort will further help us gain insights on issues like trade of between performance and cost.

REFERENCES

[1] W. C. Jakes, *Microwave Mobile Communications*, IEEE Press, New Jersey, 1974.

[2] M. Schwatz, W. R. Bennett and S. Stein, *Communication Systems and Techniques*, McGraw-Hill, New York, 1966.

[3] A. Paulraj, "Diversity Techniques" in *Mobile Communications Handbook*, J. D. Gibson, Ed., Boca Raton, CRC Press, 1996, pp. 166-176.

[4] C. M. Lo and W. H. Lam, "Performance Analysis of Bandwidth Efficient Coherent Modulation Schemes with *L*-fold MRC and SC in Nakagami-m Fading Channels", in *Personal, Indoor and Mobile Radio Communications*, pp. 572-676, Sept. 2000.

[5] A. Annamalai and C. Tellambura, "Error Rates for Nakagami-*m* Fading Multichannel Reception of Binary and *M*-ary Signals", *IEEE Transactions on Commun*., Vol. 49, pp. 58-68, Jan. 2001.

[6] M. K. Simon and M. S. Alouini, "A Unified Approach to the Performance Analysis of Digital Communication over Generalized Fading Channels", *Proceedings of the IEEE*, Vol. 86, pp. 1860-1876, Sept. 1998.

[7] M. S. Alouini and M. K. Simon, "Performance Analysis of Coherent Equal Gain Combining over Nakagami-m Fading Channels", *IEEE Transactions on Vehicular Technology*, Vol. 50, pp. 1449-1463, Nov. 2001.

[8] De Silva, C. R. C. M and M. D., Yacoub, "Bit Error Analysis of Equal Gain Combining Reception for Nakagami Fading Channels: An Exact Formulation", *Electronics Letters*, Vol. 36, pp. 1147-1149, June 2000.

[9] A. Annamalai, C. Tellambura and V. K. Bhargava, "Exact Evaluation of Maximal-Ratio and Equal-Gain Diversity Receivers for M-ary QAM on Nakagami Fading Channels", *IEEE Transactions on Commun.*, Vol. 47, pp. 1335-1344, Sept. 1999.

[10] N. Kong, T. Eng and L. B. Milstein, "A selection combining scheme for RAKE receivers", in *Universal Personal Communications*, pp. 426-430, Nov. 1995.

[11] J. S. Hammerschmidt, A. A Hutter and C. Drewes, “Comparison of Single Antenna, Selection Combining, and Optimum Combining Reception at the Vehicle”, in *Vehicular Technology Conference*, pp. 11-16, Sept. 1999.

[12] A. Annamalai, G. Deora and C. Tellambura, “Unified Error Probability Analysis for Generalized Selection Diversity in Wireless Channels”, to appear in the *IEEE Trans. On Wireless Communications*, 2003.

[13] M. K. Simon and M. S. Alouini, “A Compact Performance Analysis of Generalized Selection Combining with Independent but Nonidentically Distributed Rayleigh Fading Paths”, *IEEE Transactions on Commun.*, Vol. 50, pp. 1409-1412, Sept. 2002.

[14] A. B. Adinoyi, and S. A Al-Semari, “Performance of Coherent Schemes with Generalized Selection Combining in Rayleigh Fading”, in *Personal, Indoor and Mobile Radio Communications*, pp. 95-99, Sept. 2001.

[15] Chi Ming Lo and Wong Hing Lam, “Performance of Generalized Selection Combining for Mobile Radio Communications with Mixed Cochannel Interferers”, *IEEE Transactions on Vehicular Technology*, Vol., 51, pp. 114-121, Jan. 2002.

[16] Chyi, J. G. Proakis and C. M. Keller, “On the Symbol Error Probability of Maximum Selection Diversity Reception Schemes over a Rayleigh Fading Channel”, *IEEE Transactions on Commun*., Vol. 37, pp. 79-83, Jan. 1989.

[17] E. A. Neasmith and N. C. Beaulieu, “New Results on Selection Diversity”, *IEEE Transactions on Commun.*, Vol. 46, pp. 695-704, May 1998.

[18] A. Annamalai, “Micro-Diversity Reception of Spread-Spectrum Signals on Nakagami Fading Channels”, *IEEE Transactions on Commun.*, Vol. 47, pp. 1747-1756, Nov. 1999.

[19] Y. G. Kim and S. W. Kim, “Optimum Selection Diversity for BPSK Signals in Rayleigh Fading Channels”, *IEEE Transactions on Commun.*, Vol. 49, pp. 1715-1718, Oct. 2001.

[20] M. Nakagami, “The *m*-distribution−A General Formula of Intensity Distribution of Fading”, in *Statistical Methods in Radio Wave Propagation* ,Oxford, UK: Pergamon Press, 1960.

[21] I. S. Gradshteyn and I. M. Ryzhik, *Table of Integrals, Series, and Products*, New York: Acadamic, 1980.

[22] J. G. Proakis, *Digital Communications*, 4th ed., New York: Mcgraw-Hill, 2001.

[23] A. Annamalai and C. Tellambura, “ A New Apporach to Performance Evaluation of Generalized Selection Diversity Receivers in Wireless Channels”, in *Vehicular Technology Conference*, pp. 2309-2313, Oct. 2001.

[24] A. Annamalai, C. Tellambura and V. K. Bhargava, “Equal Gain Diversity Receiver Performance in Wireless Channels”, *IEEE Transactions on Commun*., Vol. 48, pp. 1732-1745, Oct. 2000.

[25] A. Annamalai, C. Tellambura, “Performance Evaluation of Generalized Selection Diversity Systems over Nakagami-*m* Fading Channels”, to appear in the International Journal on Wireless Communications and Mobile Computing, 2002.

[26] A. Annamalai, G. Deora and C. Tellambura, “Unified Error Probability Analysis for Generalized Selection Diversity in Ricean Fading Channels”, In *Vehicular Technology Conference* , pp. 2042-2046, May 2002.

[27] A. Annamalai, V. Ramanathan, and C. Tellambura, “Analysis of Equal Gain Diversity Receiver in Correlated Fading Channels”,' in *Vehicular Technology Conference*, pp. 2038-2041, May 2002.

[28] C. Tellambura, A. Annamalai and V. K. Bhargava, “Contour Integral Representation for Generalized Marcum q-function and its Application to Unified Analysis of Dual-branch Selection Diversity over Correlated Nakagami-m Fading Channels”, in *Vehicular Technology Conference*, pp. 1031-1034, May 2000.

ABBREVIATIONS AND NOTATIONS

ABER	average bit error rate
AWGN	additive white Gaussian noise
BPSK	binary phase shift keying
CDF	cumulative distribution function
CEP	conditional error probability
EGC	equal gain combining
GSC	generalized selection combining
LLR	log-likelihood ratio
LOS	line of sight
MGF	moment generating function
MIP	multipath intensity profile
MRC	maximal-ratio combining
PDF	probability density function
SDC	selection diversity combining
SNR	signal-to-noise ratio
WCDMA	wideband code division multiple access
UMTS	universal mobile telephony system
UWB	ultra wideband
i.i.d	independent identically distributed
i.n.d	independent non-identically distributed
αr -SDC	SDC based on LLR with phase compensation
αw-SDC	SDC based on LLR without phase compensation
α -SDC	SDC based on SNR
r-SDC	SDC based on output of match filter

VITA

Qiang Zhao was born on November 17, 1971 in Xi'an, China. He received his Bachelor of Science degree in Automatic Control from Beijing University of Aeronautics and Astronautics in July 1994. He joined in M.S. program in Electrical Engineering at Virginia Tech in August 2001 and worked as a Graduate Research Assistant at the Mobile and Portable Radio Research Group (MPRG). His research interests include performance analysis of diversity systems, channel modeling and array processing.